Atmos. Chem. Phys. Discuss., doi:10.5194/acp-2016-885, 2016
Manuscript under review for journal Atmos. Chem. Phys.
Published: 7 November 2016

Atmospheric Chemistry and Physics Discussions

Atmospheric aerosol compositions over the South China Sea: Temporal variability and source apportionment

Hong-Wei Xiao[1,2], Hua-Yun Xiao[1,2*], Li Luo[1,2*], Chun-Yan Shen[3], Ai-Min Long[4], Lin Chen[5], Zhen-Hua Long[5], Da-Ning Li[5]

[1]Laboratory of Atmospheric Environment, Key Laboratory of Nuclear Resources and Environment (Ministry of Education), East China University of Technology, Nanchang 330013, China

[2]School of Water Resources and Environmental Engineering, East China University of Technology, Nanchang 330013, China

[3]College of Fisheries, Guangdong Ocean University, Zhanjiang 524088, China

[4]State Key Laboratory of Tropical Oceanography, South China Sea Institute of Oceanology, Chinese Academy of Sciences, Guangzhou 510301, China

[5]Xisha Deep Sea Marine Environment Observation and Research Station, South China Sea Institute of Oceanology, Chinese Academy of Sciences, Sansha 573199, China

*Correspondence to: Hua-Yun Xiao (xiaohuayun@ecit.cn) and Li Luo (luoli@ecit.cn)

Abstract. Major inorganic chemical ionic concentrations (Na^+, Cl^-, SO_4^{2-}, Ca^{2+}, Mg^{2+}, K^+, NH_4^+, NO_3^-) were determined in total suspended particulates (TSP) at Yongxing Island in the South China Sea (SCS), from March 2014 to February 2015. The annual average concentration of TSP was 89.6 ± 68.0 μg/m^3, with 114.7 ± 82.1, 60.4 ± 27.0, and 59.5 ± 25.6 μg/m^3 in cool, warm, and transition seasons, respectively. Cl^- had the highest concentration, with an annual average of 7.73 ± 5.99 μg/m^3, followed by SO_4^{2-} (5.54 ± 3.65 μg/m^3), Na^+ (4.00 ± 1.88 μg/m^3), Ca^{2+} (2.15 ± 1.54 μg/m^3), NO_3^- (1.95 ± 1.34 μg/m^3), Mg^{2+} (0.44 ± 0.33 μg/m^3), K^+ (0.33 ± 0.22 μg/m^3), and NH_4^+ (0.07 ± 0.07 μg/m^3). Concentrations of TSP and the major ions showed seasonal variations, higher in the cool season and lower in the warm and transition seasons, which were influenced by wind speed, temperature, relatively humidity, rain, and air masses. Back trajectories, concentration weighted trajectories (CWT), and positive matrix factorization (PMF) of chemical compositions were analyzed for source apportionment, source contribution, and spatio-temporal variation of major ions. Back trajectories and CWTs showed that air masses at Yongxing Island were mainly from

Atmos. Chem. Phys. Discuss., doi:10.5194/acp-2016-885, 2016
Manuscript under review for journal Atmos. Chem. Phys.
Published: 7 November 2016

Atmospheric Chemistry and Physics Discussions

the northeast, southwest, and southeast in the cool, warm, and transition seasons, respectively. Na^+ and Cl^- were mainly from sea salt, which made up 74% and 82%, respectively. Asian dust contributed 50% of Ca^{2+} to the marine aerosols. Anthropogenic sources were very important for atmospheric aerosols over the island. Fossil fuel combustion (especially coal in Chinese coastal regions) was the important sources of NO_3^- (56%) and SO_4^{2-} (22%). Biomass burning in Asia accounted for 41% of K^+. 69% of NH_4^+ and 38% of SO_4^{2-} were of marine biogenic sources.

Keywords: Source apportionment; dust; biomass burning; fossil fuel combustion; marine biogenic source

1 Introduction

Aerosols or particulate matter potentially affect global atmospheric processes, chemistry, cloud formation, acid and nutrient deposition in sensitive ecosystems, and affect human health as air pollution (Deng et al., 2010; Zhang et al., 2015). Aerosols have complex sources, including primary aerosols direct from natural and anthropogenic sources, such as terrestrial dust from weathering, sea spray, biomass burning, and biological emissions. There are also secondary aerosols, which form from condensable atmospheric gases such as SO_2, NO_x, and NH_3 (Kolb and Worsnop, 2013; Xiao et al., 2012a, 2014). Therefore, aerosols are composed of various complex chemical components (Xiao and Liu, 2004) and contain sulfate, nitrate, ammonium, and mineral elements (Zhang et al., 2007). Because of rapid economic and industrial development in the last few decades, many aerosols and their precursors released by human activities have become a major environmental problem worldwide (Kolb and Worsnop, 2013). Aerosols from anthropogenic emissions can be transported long distances from polluted regions to remote open oceans, which is well recognized as a major pathway for the supply of anthropogenic material to ocean surface waters (Duce et al., 2008; Lawrence and Lelieveld, 2010; Jung et al., 2012).

Atmospheric aerosol deposition over remote open oceans can increase ocean productivity and carbon sequestration (Duce et al., 2008; Kim et al., 2014; Landing and Paytan, 2010), but aerosol input to such oceans varies considerably in both time and space. Such variations are modulated by sources, chemical processes, and environmental parameters, e.g., wind and temperature (Landing and Paytan, 2010; Xiao et al., 2015). Time-series measurements of aerosol particles over the subarctic Northeast Pacific Ocean have indicated that major contributions to the aerosol mass were from the oxidation of dimethyl sulfide (DMS), sea salt, and ship emissions (Phinney et al., 2006). High NH_4^+ and NO_3^- concentrations have been found in North and South Pacific Ocean when air masses were derived from the Asian continent and the Kamchatka Peninsula, whereas low concentrations were observed when air masses were from the central Pacific Ocean (Jung et al., 2012); therefore, NH_3 and NO_x are influenced by both natural and anthropogenic sources. In the North Sea, the anthropogenic fraction is lower for

Atmos. Chem. Phys. Discuss., doi:10.5194/acp-2016-885, 2016
Manuscript under review for journal Atmos. Chem. Phys.
Published: 7 November 2016

air masses from the North Atlantic than for those from the European continent (Ebert et al., 2000). There are four discrete transport regimes over the western North Atlantic Ocean at Bermuda that affect the sources (Keene et al., 2005). The East China Sea was more influenced by Asian dust storms whereas the Yellow Sea was more influenced by human activities, during March and April, 2011 (Zhao et al., 2015). Dust from the Gobi Desert with pollutants from eastern China transports numerous dust elements and secondary pollutants to the South China Sea (SCS) (Liu et al., 2014).

The SCS is in the tropical–subtropical rim of the Northwest Pacific Ocean and is one of the largest marginal seas in the world (Fig. 1). The SCS is adjacent to several rapidly growing Asian economies, including China, the Philippines, Malaysia, Vietnam, and Indonesia (Kim et al., 2014). Consequently, the sea receives substantial amounts of aerosols from surrounding regions through long-range atmospheric transport (Fig. 1; Atwood et al., 2013; Jung et al., 2012). The SCS has a monsoon climate, with a northeast monsoon in winter and spring and a southwest monsoon in summer and autumn (Cui et al., 2016). Thus, aerosol optical thickness (AOT) shows spatial and seasonal variations, with higher AOT in the northern SCS during the cool season and higher AOT in the southern SCS in the warm season (Fig. 1). The SCS receives dust and pollutions from the northeast SCS in winter and spring, e.g., from China and Japan (Wang et al., 2013; Xiao et al., 2015); during summer and autumn, the SCS receives aerosols and pollutants from biomass burning in the southwest of SCS, e.g., from Malaysia and Indonesia (Atwood et al., 2013). According to Lawrence and Lelieveld (2010), emissions of SO_2 and NO_x in Northeast Asia are mainly from fossil fuel combustion and industrial processes, and from fossil fuel combustion and biofuel burning in South Asia. Biomass burning in Asian countries is an important contributor to aerosol deposition in the SCS (Streets et al., 2003).

To get better understanding of potential sources, source contributions, and spatio-temporal variations of marine aerosols over the SCS, total suspended particulate (TSP) were continuously collected at Yongxing Island from March 2014 to February 2015. The concentrations of major inorganic water-soluble ions were determined. Furthermore, back trajectories, concentration-weighted trajectory (CWT) and positive matrix factorization (PMF) analyses were also used to identify and apportion the main sources of aerosols and their chemical composition over the SCS.

2 Materials and Methods

2.1 Study site

Atmos. Chem. Phys. Discuss., doi:10.5194/acp-2016-885, 2016
Manuscript under review for journal Atmos. Chem. Phys.
Published: 7 November 2016

Atmospheric Chemistry and Physics Discussions

Aerosol samples were collected from March 2014 through February 2015 on the rooftop of Xisha Deep Sea Marine Environment Observation and Research Station, South China Sea Institute of Oceanology, Chinese Academy of Sciences (SCSIO, CAS). This station is at the Yongxing Island (YXI, Fig. 1; 16.83°N, 112.33°E). This island has a tropical monsoon climate, with northeast monsoon in winter and spring, and southwest monsoon in summer and autumn (Xiao et al., 2015). The island is located in the high aerosol concentrations area of the northern SCS during winter and spring, and also at the periphery of such concentrations area of the southern SCS during summer and autumn (Fig. 1). Therefore pollutants can be from Northeast Asia in winter and spring, and Southeast Asia in summer and autumn. It is also influenced by local SCS marine sources. More information about Yongxing Island is given elsewhere (Xiao et al., 2015 and 2016). In the present study, it was divided into three seasons according to wind direction and back trajectories. The cool season was March, April, October, November, December 2014 and January, February 2015, with principal air masses from the northeast, and the warm season was June–September 2014, with air masses major from the southwest. The transition season was May 2014, with major air masses from the local southeast. Yongxing Island has an annual average temperature of 27.7 ± 2.7 °C, relative humidity (RH) of 80 ± 7%, and wind speeds of 3.6 ± 1.8 m/s. There were strong seasonal variations between March 2014 and February 2015 (Fig. 2). Annual rainfall was 1526 mm during this period, with about 30% occurring in the cool season (Fig. 2).

2.2 Sample collection and chemical analyses

Aerosol was collected on quartz filters (8 × 10 inch, Tissuquartz™ Filters, 2500 QAT-UP, Pallflex, Washington, USA) using a special high-flow rate (1.05 ± 0.03 m^3/min) KC-1000 sampler (Laoshan Institute for Electronic Equipment, Qingdao, China). The sampling time was nominally 96 hours (4 days one sample). All samples were stored in a refrigerator at −20°C until analysis in the laboratory.

In the laboratory, one eighth filters were cut and placed in a clean 50-ml Nalgene tube with additional 35-ml ultrapure water. These tubes were washed for 30 minutes using ultrasonic vibration. They were then shaken for 30 minutes on a horizontal shaker at a rate of ~300 rpm and left to rest for an another 30 minutes at room temperature. The extract was filtered using pinhole filters, which were then rinsed twice with 5-ml ultrapure water. The extract and rinse were put into 50-ml tubes together and stored in a refrigerator at −20 °C until chemical analyses.

Major anion concentrations (F^-, Cl^-, NO_3^-, SO_4^{2-}, Br^-) were determined by ICS-90 ion chromatography (Dionex, California, USA). Water-soluble metal and nonmetal elemental concentrations (Al, Ca, Fe, K, Mg, Mn, Na, SiO_2, Sr) were analyzed by an MPX inductively coupled plasma optical emission spectrometer (ICP-OES, Vista, CA,

Atmos. Chem. Phys. Discuss., doi:10.5194/acp-2016-885, 2016
Manuscript under review for journal Atmos. Chem. Phys.
Published: 7 November 2016

Atmospheric Chemistry and Physics Discussions

USA). NH_4^+ concentration was determined by spectrophotometry after treatment with Nessler's reagent. The detection limits of F^-, Cl^-, NO_3^-, SO_4^{2-}, Br^- were 0.03, 0.03, 0.08, 0.075 and 0.1 mg/L, respectively, and the relatively standard deviation of these ions were 0.57%, 2.55%, 1.16%, 1.36% and 11.36%, respectively (Xiao et al., 2013 and 2016). The detection limits of Al, Ca, Fe, K, Mg, Mn, Na, SiO_2, Sr were 0.025, 0.003, 0.002, 0.06, 0.0005, 0.0005, 0.02, 0.015 and 0.00008 mg/L, respectively, and the relatively standard deviation of these ions were less than 1.5% (Xiao et al., 2013 and 2016). The detection limit of NH_4^+ was 0.1 mg/L and its relatively standard deviation was less than 5.0% (Xiao et al., 2013 and 2016). In this study, Al in most of samples was less than the detection limit.

2.3 Back trajectories and CWT analysis

Back trajectories and CWT are used to determine the long-distance transport of atmospheric pollutants and regional source areas. Detailed principles of back trajectories and CWT were given in our previous studies (Xiao et al., 2014; Xiao et al., 2015). For each day, 10-day (240 hours) back trajectories of air masses arriving at Yongxing Island were computed. CWT modeled TSP, and Ca^{2+}, Mg^{2+}, K^+, SO_4^{2-}, NO_3^- and NH_4^+ concentrations at the island. The region from 70°E to 160°E and from 20°S to 60°N was defined as the source domain based on back trajectories during the sampling period, containing 14,400 grid cells of 0.5° × 0.5°.

2.4 PMF model

PMF is an effective source apportionment receptor model that does not require source profiles prior to analysis and has no limitation on source numbers (Tiwari et al., 2013; Zhang et al., 2015). The principles of PMF are detailed elsewhere (Han et al., 2006; Hien et al., 2004; Schmale et al., 2013; Yu et al., 2013). In our study, PMF 5.0 (United States Environmental Protection Agency) was used to determine source apportionment of TSP and each major ion based on TSP, F^-, Cl^-, NO_3^-, SO_4^{2-}, Ca, K, Mg, Mn, Na, and Sr. Five physically realistic sources for TSP and major ions were identified, i.e., sea salt, crust, biomass burning, fossil fuel combustion, and marine biogenic.

3 Results and Discussion

3.1 Aerosol chemical composition over SCS and comparison with global marine aerosols

3.1.1 Aerosol characteristics over SCS

Figures 3 and 4 provide information on atmospheric concentrations of TSP aerosols and major inorganic ions during the sampling period at Yongxing Island. The annual average TSP concentration at the island was 89.6 ±

Atmos. Chem. Phys. Discuss., doi:10.5194/acp-2016-885, 2016
Manuscript under review for journal Atmos. Chem. Phys.
Published: 7 November 2016

Atmospheric Chemistry and Physics Discussions

68.0 μg/m^3, with a range of 16.4 to 440.1 μg/m^3. This TSP level is much lower than cities around the world (Wang et al., 2006; Xiao and Liu, 2004; Deng et al., 2011; Naga et al., 2014). It is also lower than some remote sites, such as Mountain Tai (Deng et al., 2011). Of course, it is higher than lots of remote sites, such as Tianchi, Qinghai Lake (Deng et al., 2011; Zhang et al., 2014).

The major inorganic ionic concentrations (Na^+, Cl^-, SO_4^{2-}, Ca^{2+}, Mg^{2+}, K^+, NH_4^+, and NO_3^-) accounted for 24.8% of TSP. Cl^- had the highest concentration among these ions, from 0.39 to 36.47 μg/m^3, with an annual average of 7.73 ± 5.99 μg/m^3. It was followed by SO_4^{2-} (range 0.52–23.34 μg/m^3, average 5.54 ± 3.65 μg/m^3), Na^+ (0.9 –8.86 μg/m^3, average 4.00 ± 1.88 μg/m^3), Ca^{2+} (0.17–9.65 μg/m^3, average 2.15 ± 1.54 μg/m^3), NO_3^- (0.10–10.05 μg/m^3, average 1.95 ± 1.34 μg/m^3), Mg^{2+} (0.02–1.55 μg/m^3, average 0.44 ± 0.33 μg/m^3), K^+ (0.06–1.13 μg/m^3, average 0.33 ± 0.22 μg/m^3), NH_4^+ (0.01–0.32 μg/m^3, average 0.07 ± 0.07 μg/m^3) (Fig. 3).

3.1.2 Aerosols over SCS compared with global marine aerosols

The annual average TSP concentration at Yongxing Island is also lower than those in the northern Yellow Sea (123.2 μg/m^3), another Chinese marginal sea (Wang et al., 2013). However, the mean TSP concentration at Yongxing Island is not lower than other remote islands or seas, such as the Indian and Pacific oceans and three islands of Okinawa (Arakaki et al., 2014; Balasubramanian et al., 2013; Zhang et al., 2010; Zhang et al., 2014).

The aforementioned annual average concentrations and orders of ionic concentration are comparable with those reported in many remote oceans (Fig. 5), e.g., Hedo, which is at the junction of the East China Sea and Northwest Pacific. The marine ions (Na^+ and Cl^-) accounted for 53% of total major ions (Fig. 4). Na^+ and Cl^- concentrations at Yongxing Island were higher than most reported values in global ocean and remote sites (Fig. 5), such as the Indian Ocean, Arabian Sea, Oki and Rishiri islands in the Sea of Japan, Amsterdam Island in the Southern Ocean, Bermuda in the Atlantic Ocean, and Hawaii in the Pacific. However, Na^+ and Cl^- concentrations were lower than samples from cruises, such as over the southern Atlantic and Pacific. The Ca^{2+} concentration was the highest in all global oceans and composed 10% of major ions, followed by the Mediterranean Sea, southern Atlantic and northern Atlantic-2 (Fig. 5). The relatively high Ca^{2+} concentration may be because of Asian terrestrial dust transported to Yongxing Island and dust from local weathered dead coral from Yongxing Island development (Xiao et al., 2016). As a tracer for dust, non-sea salt Ca^{2+} (nss-Ca^{2+}) accounted for 93% of total Ca^{2+}, ranging from 0.14 to 9.31 μg/m^3 with an annual average of 1.99 μg/m^3. Large contributions of nss-Ca^{2+} were also found in the Mediterranean Sea, southern Atlantic and northern Atlantic-2, being at 88.4%, 90.3% and 90.0%, respectively (Zhang et al., 2010). The relatively high nss-Ca^{2+} concentrations were potentially from the crust or dust from the

Atmos. Chem. Phys. Discuss., doi:10.5194/acp-2016-885, 2016
Manuscript under review for journal Atmos. Chem. Phys.
Published: 7 November 2016

Atmospheric Chemistry and Physics Discussions

Sahara Desert (Zhang et al., 2010). Comparing Yongxing Island with global oceans, average Mg^{2+}concentrations were nearly consistent with those of Na^+ (Fig. 5). K^+ was also the highest among the global oceans (Fig. 5). As a tracer for biomass/biofuel burning, nss-K^+ ranged from 0 to 0.87 μg/m^3, with an annual average of 0.18 μg/m^3 and a contribution of 55% to total water soluble K^+ at Yongxing. In general, SO_4^{2-}, NO_3^- and NH_4^+ were major in the form of secondary inorganic aerosols. They accounted for only 34.0% of total inorganic ionic concentrations, giving them an intermediate position among the global ocean (Fig. 5). The average SO_4^{2-}concentration at Yongxing was the highest among those in the global ocean. As shown in Fig. 4, the mean contribution of SO_4^{2-} to major inorganic ionic components was ~ 25% at Yongxing. The nss-SO_4^{2-} concentration was 3.66 μg/m^3, with a contribution of 66.1% to total SO_4^{2-}. Similar to SO_4^{2-}, the average concentration of NO_3^- in this study was the highest among those in the global ocean. It accounted for 9% of major ions at Yongxing Island. This indicates that a large number of anthropogenic sources affected the concentrations of SO_4^{2-} and NO_3^-. It was surprising that NH_4^+ had relatively low concentrations over most oceans, except for the southern Atlantic and Mediterranean Sea (Fig. 5). The average NH_4^+ concentration was 0.07 ± 0.07 μg/m^3 in aerosol at Yongxing Island (Fig. 3), representing < 1% of total major ions (Fig. 4). Further, low concentrations of NH_4^+ were also observed in rainwater on the island (Xiao et al., 2016).

3.1.3 Global marine aerosol chemical patterns

Globally, sea salt ions (Na^+ and Cl^-) were the most important components in marine atmospheric aerosol, with higher concentration of Cl^- than Na^+, except over the Mediterranean and North seas (Fig. 5). In the marine atmosphere, sea salt aerosol (NaCl) can react with sulfuric acid and nitric acid to release HCl, which results in a deficit of Cl^- relative to Na^+ (Zhang et al., 2010). It is also found that a deficit of Cl^- in transition season at Yongxing Island (Fig. 4). For SO_4^{2-} with ss-SO_4^{2-} and nss-SO_4^{2-}, nss-SO_4^{2-} was greatly influenced by anthropogenic sources from developed industrial areas, leading to higher concentrations of SO_4^{2-} than Na^+ and Cl^-. Examples were Bermuda, Ogasawara, and the Arabian Sea (Fig. 5), where nss-SO_4^{2-} was the preferred species for acid displacement (Zhang et al., 2010). As another import ion of anthropogenic sources, NO_3^- concentrations were often consistent with those of nss-SO_4^{2-} (Zhang et al., 2010), with relatively high concentrations among major ions (Fig. 5). Relatively high concentrations of SO_4^{2-} and NO_3^- were also found over the SCS. NH_4^+ had the lowest concentrations among the major ions in most marine atmospheric aerosols, suggesting that little ammonia transport to the open ocean, such as Yongxing Island. However, there were some exceptions. For example, the southern Atlantic and Mediterranean Sea had the highest NH_4^+ concentrations among major ions (Fig. 5). Over most seas, the order was $Ca^{2+} > Mg^{2+} > K^+$. However, we found that Mg^{2+} had higher concentrations than Ca^{2+} in some remote ocean areas,

Atmos. Chem. Phys. Discuss., doi:10.5194/acp-2016-885, 2016
Manuscript under review for journal Atmos. Chem. Phys.
Published: 7 November 2016

Atmospheric Chemistry and Physics Discussions

such as in the Pacific, Atlantic and Southern oceans. This indicates that Ca^{2+} of crustal origin was difficult to transport to the remote oceans, and Mg^{2+} may mainly be from sea salt over the open ocean (Moody et al., 2014).

3.2 Seasonal patterns of aerosol chemical species over SCS and adjacent areas

3.2.1 Seasonal characteristics at Yongxing Island

As illustrated in Figs. 4 and 6, seasonal and monthly TSP concentrations and major inorganic water-soluble ion concentrations had distinctive features at Yongxing Island. Generally, concentrations of TSP and major inorganic ions were higher in the cool season than in the warm season (Fig. 6). Seasonal variations were the same as those in most other studies (Arakaki et al., 2014; Wang et al., 2006; Xiao and Liu, 2004; Zhang et al., 2012).

Average TSP concentrations were 114.7 ± 82.1, 60.4 ± 27.0 and 59.5 ± 25.6 μg/m^3 in the cool, warm and transition seasons, respectively, with the highest monthly average in November 2014 and the lowest in April (39.4 μg/m^3) and September (39.9 μg/m^3) of that year (Fig. 6). There were lower concentrations in the warm season than in the cool season, because rainfall at Yongxing Island concentrates in the former season (Fig. 2), being the same as many other studies (Wang et al., 2006; Zhao et al., 2015). However, there was no relationship between TSP concentration and rainfall ($p > 0.05$; Table 1), indicating that rainfall is not a major factor controlling seasonal variation of that concentration. The positive correlation between TSP concentration and wind speed ($p < 0.01$) shown in Table 1 suggests that relatively strong speeds can produce many particles from both sea spray and terrigenous matter. We discovered negative correlations between TSP concentration and temperature ($p < 0.01$) and relatively humidity ($p < 0.01$) (Table 1), indicating that warm temperatures and high relatively humidity enhance particle wetting and interaction. Figure S1 also shows that meteorological parameters affected the major ions, with wind speed having a positive influence and relatively humidity, temperature and rainfall a negative one. Based on the arrow lengths in the figure, rainfall had less effects on major ions than others.

As shown in Figs. 4 and 6, sea salt ions Na^+ and Cl^- were characterized by a gradual increase from the transition to cool season. Their concentrations (in μg/m^3) in the cool, warm and transition seasons were 4.91 ± 1.82 and 3.04 ± 1.08, 2.28 ± 1.35 and 9.93 ± 6.78, and 5.25 ± 2.63 and 3.73 ± 3.63, respectively, with corresponding contributions of 52%, 57% and 57% to total major ions in those seasons. The highest Na^+ and Cl^- concentrations in a single sample were found in November, with the lowest concentrations in May and April, respectively. The highest average monthly concentrations were in November. Positive relationships between Na^+ or Cl^- and wind speed in Table 1 ($p < 0.01$, correlation coefficient $R = 0.44$ and $p < 0.01$, $R = 0.43$, respectively) and small angles (<< 90^o) between Na^+ or Cl^- and wind speed (long arrows) in Fig. S1 at Yongxing Island suggest that sea salt concentrations

Atmos. Chem. Phys. Discuss., doi:10.5194/acp-2016-885, 2016
Manuscript under review for journal Atmos. Chem. Phys.
Published: 7 November 2016

Atmospheric Chemistry and Physics Discussions

were dependent on wind speed. This is consistent with results at Chichijima Island (Boreddy and Kawamura, 2015). There was a negative relationship between Na^+ and rainfall ($p < 0.05$) but no relationship between Cl^- and rainfall ($p > 0.05$), showing that Na^+ mainly existed in coarse particles and was readily removed by rainfall (Fig. S1). As shown in Table 1 and Fig. S1, concentrations of Na^+ and Cl^- were also negatively influenced by temperature and relatively humidity.

As shown in Fig. 6, the highest monthly average concentrations of Ca^{2+} were in February. Its monthly trends were different from those of TSP, Na^+ and Cl^-, suggesting that Ca^{2+} from terrestrial dust sources may be influenced by different factors. Ca^{2+} accounted for 10%, 13% and 8% of total major ions in the cool, transition and warm seasons, respectively (Fig. 4). There was no correlation between Ca^{2+} and wind speed, in contrast with TSP, Na^+ and Cl^- (Table 1). However, there was a negative relationship between Ca^{2+} and rainfall ($p < 0.05$; Table 1 and Fig. S1). These results suggest that Ca^{2+} existed in coarse particles that can be readily removed by rainfall, the same as Na^+. Thus, a low mass concentration was observed for Ca^{2+} in the rainy (warm) season (Fig. 6), with a low percentage being in the warm season in Fig.4.

Although Mg^{2+} is often treated as crustal-derived ions and elements in continental studies (Zhang et al., 2015), its highest monthly average concentrations were in November at Yongxing Island, the same as Na^+ and Cl^- (Fig. 5). As shown in Fig. 5 and Table 1, similar trends and strong correction were observed among Na^+, Cl^- and Mg^{2+}, suggesting that Mg^{2+} may mainly derive from sea salt rather than continental sources. However, there were no relationships between Mg^{2+} and wind speed, temperature, relatively humidity, or rainfall (Table 1), in contrast to other ions, such as Na^+ and Cl^-. These results reveal that Mg^{2+} has complex sources or behaviors in the marine atmosphere at Yongxing Island. The same phenomenon was found in rainwater (Xiao et al., 2016). Moody et al. (2014) suggested that Na^+ may exist in super-micron size aerosols, whereas Mg^{2+} in sub-micron size aerosols are slightly influenced by meteorological parameters.

As a tracer for biomass burning, K^+ concentrations were 0.42 ± 0.23 μg/m^3 in the cool season, 0.22 ± 0.18 μg/m^3 in warm season, and 0.15 ± 0.07 μg/m^3 in the transition season at Yongxing, with the maximum monthly average concentrations in February and the minimum in July (Fig. 6). However, the lowest nss-K^+ monthly average concentration was in August. The results show that nss-K^+ is derived from Chinese biomass/biofuel burning in the cool season (Lawrence and Lelieveld, 2010). Streets et al. (2003) computed that China contributes 25% of total biomass burning in Asia. Many sites in Chinese coastal regions had higher K^+ and nss-K^+ concentrations than those at Yongxing Island (Wang et al. 2006), further indicating that Chinese and other Northeast Asian regions' biomass/biofuel burning have a strong influenc on atmospheric composition over the SCS.

Atmos. Chem. Phys. Discuss., doi:10.5194/acp-2016-885, 2016
Manuscript under review for journal Atmos. Chem. Phys.
Published: 7 November 2016

Atmospheric Chemistry and Physics Discussions

Biomass/biofuel burning releases not only K^+ but also SO_2 and NO_x (Lawrence and Lelieveld, 2010). Furthermore, considerable fossil fuel burning and industrial processes generate large amounts of SO_2 and NO_x in northern Asia (Lawrence and Lelieveld, 2010), resulting in the transport of substantial secondary inorganic aerosols containing SO_4^{2-} and NO_3^- to the SCS. Therefore, similar to K^+, the highest monthly concentrations of SO_4^{2-} and NO_3^- were observed in February, being at 13.08 ± 9.04 and 4.99 ± 4.33 μg/m^3, respectively (Fig. 6). As shown in the figure, SO_4^{2-} concentrations in the cool and warm seasons were 7.22 ± 3.92 and 3.26 ± 1.26 μg/m^3, respectively, accounting for 26% and 22% of total major ions, and NO_3^- concentrations were 2.43 ± 1.54 and 1.30 ± 0.64 μg/m^3, accounting for 9% and 9%. NO_x emission from fossil fuel combustion made up 61% and 76% of total NO_x emission in southern and northern Asia, respectively, and SO_2 from the same source made up 77% and 75% (Lawrence and Lelieveld, 2010). According to the aerosol $\delta^{15}N\text{-}NO_3^-$ at Yongxing Island, NO_3^- mainly came from coal combustion in China during the cool season, and from natural emissions during the warm season (Xiao et al., 2015). In recent years, NO_x emission has also increased greatly because of increasing energy demand, although coal-fired power plants have been restricted (Zhao et al., 2015).

The NH_4^+ showed maxima in the cool season and minima in the warm season, being 0.08 ± 0.08 and 0.04 ± 0.03 μg/m^3, respectively. Atmospheric NH_x is usually rapidly deposited near source regions and has a short residence time, about several hours in the marine boundary layer (Boreddy and Kawamura, 2015; Xiao et al., 2012a; Xiao and Liu, 2002). Thus, NH_x transportation from continental to remote sea sites is difficult. Therefore, NH_4^+ in aerosol at Yongxing Island was possibly from marine biogenic emissions, as being reported at other marine sites (Altieri et al., 2014; Jickells et al., 2003).

3.2.2 Seasonal patterns over SCS and adjacent areas

The spatial variability in seasonal patterns of the major inorganic ionic components at Yongxing Island and adjacent sites of Acid Deposition Monitoring Network in East Asia (EANET) is portrayed in Fig. 7. In general, total major inorganic ionic concentrations tended to be higher in cool seasons and lower in warm seasons to the north of Phnom Penh, including Phnom Penh, Hoa Binh, Hanoi, Hongwen, Hedo, Ogasawara, and Yongxing Island, consistent with previous studies (Boreddy and Kawamura, 2015; Wang et al., 2006; Xiao and Liu, 2004). There was no substantial seasonal variation at other sites of EANET, and there was no strong seasonal variation of rainfall there either. These results suggest that rainfall and wind patterns influence the ionic seasonal variations (Lawrence and Lelieveld, 2010; Wang et al., 2006; Xiao et al., 2013; Xiao and Liu, 2004). Additionally, total major ionic concentrations were higher in the north than in the south, indicating more anthropogenic pollutants in the north,

Atmos. Chem. Phys. Discuss., doi:10.5194/acp-2016-885, 2016
Manuscript under review for journal Atmos. Chem. Phys.
Published: 7 November 2016

Atmospheric Chemistry and Physics Discussions

such as SO_4^{2-} and NO_3^- (Lawrence and Lelieveld, 2010). As it is well known, the most densely populated regions in the north, including Hanoi, northeastern China, Pearl River Delta of China, Korea, and Japan release large amounts of pollutants (Lawrence and Lelieveld, 2010), which then transport to the SCS in the cool seasons (Fig. 1).

The total ionic concentrations were higher at the three islands than sites to the south of Phnom Penh. As shown in Fig. 7, relatively high concentrations of Na^+ and Cl^- were found at those islands, suggesting that ions from sea salt had large contributions to total major ions, i.e., 52.8%, 62.5% and 55.6% at Yongxing, Ogasawara and Hedo, respectively. This represents high mass concentrations of sea salt in the marine atmospheric aerosol. The highest concentrations of both Na^+ and Cl^- appeared in November at Yongxing and Hedo islands, which were influenced by a strong northeast monsoon. The highest concentrations of both Na^+ and Cl^- were in September at Ogasawara Island, which were influenced by a strong southeast monsoon from the Pacific. The relationship between Na^+, Cl^- and wind speed at Yongxing ($p < 0.01$) is shown in Table 1 and Fig. S1. Other sites in Fig. 7 were also influenced by wind speed and winds directly from the ocean. However, the highest Na^+ and Cl^- concentrations at some sites did not appear in the same month, e.g., at Hongwen, the highest concentrations of Na^+ were in April and the highest of Cl^- were in January. Excess Cl^- in January there may have come from biomass burning and coal combustion in China (Duan et al., 2006).

The highest concentrations of Mg^{2+} were in the same months as Na^+ at most sites, indicating that Mg^{2+} may be from sea salt with Na^+. The exceptions were at Hoa Binh and Tanah Rata with the maximum Mg^{2+} concentrations being in December and July, respectively. This suggests that Mg^{2+} originates from the crust rather than oceans (Xiao and Liu, 2004), or from both crust and oceans at these sites. Hoa Binh was influenced by the northeast monsoon, which carries strongly weathering crustal matters from China Yunnan-Guizhou Plateau karst (Hien et al., 2004; Xiao et al., 2013), and there was a strong relationship between Mg^{2+} and Ca^{2+} ($R = 0.7$, $p < 0.05$). Ca^{2+}, a tracer for dust, had its highest concentrations in July at Phnom Penh, Tanah Rata, Petaling Jaya, Serpong, and Danum Valley, all of which are located in the south of the SCS. In these regions, relatively little rainfall (rainfall data from EANET) and strong sunlight were observed in that month, leading to strong weathering that generated Ca^{2+}. However, the highest Ca^{2+} concentrations were found at other sites in the cool season, during which there was much dust from Northeast Asia (Fig. S2; Boreddy and Kawamura, 2015; Liu et al., 2014; Wang et al., 2011). This result is consistent with earlier studies (Boreddy and Kawamura, 2015; Cheng et al., 2000; Liu et al., 2014; Zhao et al., 2015). The Ca^{2+} data also proved that Asian dust can affect the northern SCS, but it is difficult for Asian dust to be transported to the southern SCS (Figs. 1 and S2).

Atmos. Chem. Phys. Discuss., doi:10.5194/acp-2016-885, 2016
Manuscript under review for journal Atmos. Chem. Phys.
Published: 7 November 2016

Atmospheric Chemistry and Physics Discussions

Figure 8 shows fire spot data from MODIS global fire mapping around the SCS during March 2014 through February 2015. Additionally, dynamic smoke surface concentrations every day in that period and region is shown in Fig. S2. The fire spot and smoke data give information on seasonal variations of biomass burning around the SCS. This activity was strong from January to April in the west of the SCS, including Vietnam, Thailand and Laos, and between July and October in the south of the SCS, including Malaysia and Indonesia (Figs. 8 and S2). These data are consistent with other studies showing substantial monthly CO emissions from biomass burning during February–April and August–October in Southeast Asia, and February–May in southern China and Taiwan (Streets et al., 2003). K^+ is commonly used as a tracer of biomass and biofuel burning (Deng et al., 2010). As shown in Fig. 7, we found that the maximum K^+ was in the aforementioned months at most sites, suggesting that Asian biomass burning heavily influenced the SCS region.

Biomass burning is an important source of atmospheric pollutants, such SO_2, NO_x, and NH_3 (Streets et al., 2003). According to the reported by Streets et al. (2003), emissions of biomass burning in Asia contribute 0.37 Tg of SO_2, 2.8 Tg of NO_x, and 0.92 Tg of NH_3, or 1.1%, 11% and 3.3% of total Asian emissions, respectively. Natural emissions include SO_2 and NH_3 from marine and soil biological processes (Altieri et al., 2014; Boreddy and Kawamura, 2015; Xiao et al., 2012a), and NO_x from those processes and lightning (Price et al., 1997; Xiao et al., 2015). Certainly, fossil fuel combustion, industrial processes, biofuel burning, agricultural and waste handling also generate large quantities of SO_2, NO_x, NH_3 in Asia (Lawrence and Lelieveld, 2010; Liu et al., 2013; Xiao et al., 2012a; Xiao et al., 2014; Xiao et al., 2015). In general, the three marine sites (Yongxing, Hedo, and Ogasawara islands) had smaller proportions of SO_4^{2-}, NO_3^- and NH_4^+ than inland sites, with the three ions accounting for ~35% at the marine sites and up to 65% at the other sites. This indicates that anthropogenic contributions are smaller over remote open oceans than at continental sites. Figure 6 shows that the highest SO_4^{2-}, NO_3^- and NH_4^+ concentrations were found during the cool season in the north of Phnom Penh, including Phnom Penh, Hoa Binh, Hanoi, Hongwen, Hedo, Ogasawara, and Yongxing, consistent with total inorganic major ions. This indicates that the pollutants from Northeast Asia have a great impact on the Northwest Pacific. Figure S2 confirms these findings. We also found that most sites in the south of Phnom Penh had maximum SO_4^{2-} and NO_3^- concentrations in the same months as the highest K^+ concentrations occurred, suggesting that biomass and biofuel burning are important sources for SO_4^{2-} and NO_3^- in those regions. Lawrence and Lelieveld (2010) found that such burning was important in the emissions of SO_4^{2-} and NO_3^- in southern Asia, whereas fossil fuel combustion and industrial processes tended to be dominant in northern Asia (Xiao et al., 2015). However, maximum NH_4^+ concentrations at some sites (e.g., Petaling Jaya, Serpong, Danum Valley) were inconsistent with SO_4^{2-} and NO_3^-. Moreover, there was no relationship between

Atmos. Chem. Phys. Discuss., doi:10.5194/acp-2016-885, 2016
Manuscript under review for journal Atmos. Chem. Phys.
Published: 7 November 2016

Atmospheric Chemistry and Physics Discussions

SO_4^{2-} or NO_3^- and NH_4^+ at these sites in the south of Phnom Penh, including Phnom Penh and Yongxing Island (both $p > 0.05$). The results are inconsistent with previous studies (Boreddy and Kawamura, 2015; Hsu et al., 2007; Wang et al., 2006; Xiao et al., 2013; Xiao and Liu, 2004). In the marine atmosphere, H_2SO_4 and HNO_3 can react with NaCl to generate Na_2SO_4, $NaNO_3$ in coarse particles, and HCl (Boreddy and Kawamura, 2015; Xiao et al., 2015). NH_4^+ is often predominant in fine particles and may exist in the form of $(NH_4)_2SO_4$ in their accumulation (Ooki et al., 2007; Ottley and Harrison, 1992). However, ratios of NH_4^+ to nss-SO_4^{2-} in the size range D > 0.22 μm (D = diameter) decreased with particle size (Ooki et al., 2007). Ooki et al. (2007) found that in the range 0.06 < D < 0.22 μm, $(NH_4)_2SO_4$ was mainly derived from marine biogenic sources. In addition, ammonium salts such as NH_4Cl and NH_4NO_3 are readily dissociable by evaporation in the marine atmosphere (Ottley and Harrison, 1992), which caused a weak relationship between NH_4^+ and other ions at Yongxing Island.

3.3 Aerosol chemical principal component analysis

3.3.1 Correlation analysis

Correlation analysis was used to characterize relationships among the ions and distinguish potential sources of ionic constituents (Xiao et al., 2013; Xiao and Liu, 2004). As shown in Table 1, *p*-values among all ions except NH_4^+ were < 0.01 at Yongxing Island, indicating that the correlation between each two ions was statistically significant. *R* between Na^+ and Cl^- was > 0.8, suggesting that they have a major common source and may exist in NaCl within aerosols in the marine atmosphere. The mole equivalent ratios of Cl^-/Na^+ (neq/L) in aerosols were slightly larger than seawater in annual, cool and warm seasons at Yongxing Island (Table 2). This suggests that Cl^- enrichment had an anthropogenic or natural biomass burning origin (Duan et al., 2006; Jung et al., 2012; Xiao et al., 2013). However, as shown in Table 2, the ratio of Cl^-/Na^+ was slightly smaller than seawater in the transition season, most likely because air masses were primarily from local areas far from the continent (Fig. 1), where wind is weak (Fig. 2). Thus, Cl^- depletion occurred through the volatilization of HCl during the reaction of NaCl with N_xO_y, HNO_3, or H_2SO_4 (Hsu et al., 2007; Jung et al., 2012; Xiao et al., 2015). Nevertheless, most Na^+ originates from sea salt, but part is from dust, fossil combustion, and biomass burning (Tiwari et al., 2013; Xiao et al., 2016; Zhang et al., 2015). There was a strong relationship between K^+ and Cl^- (Table 1), indicating that KCl is partly from sylvite weathering and biomass burning (Xiao et al., 2013). In addition, K^+ had strong correlation with Ca^{2+}, implying that they may come from crustal components. According to the ratio of K^+/Na^+ at Yongxing Island and in seawater (Table 3), a part of K^+ is from seawater. Further, a strong relationship between K^+ and SO_4^{2-} was found (Table 1), indicating that they have a common source, i.e., biomass burning (Li et al., 2003; Streets et al., 2003).

Atmos. Chem. Phys. Discuss., doi:10.5194/acp-2016-885, 2016
Manuscript under review for journal Atmos. Chem. Phys.
Published: 7 November 2016

Atmospheric Chemistry and Physics Discussions

There was also a strong relationship between Ca^{2+} and SO_4^{2-}, meaning that they may exist in the form of $CaSO_4$ in the marine atmosphere. The secondary aerosols SO_4^{2-} and NO_3^- were also strongly correlated, which may be attributed to similarity of their chemical behavior and a common source of their precursors SO_2 and NO_x (Xiao et al., 2013). Ratios of Mg^{2+}/Na^+ were equal to those of seawater throughout the year at Yongxing (Table 2), indicating that most Mg^{2+} was likely from sea salt. However, *R* between Mg^{2+} and Na^+ was much smaller than that between Cl^- and Na^+, suggestive of a different behavior of Mg^{2+} to that of Na^+. The ratios of $NO_3^-/nss\text{-}SO_4^{2-}$ and $NH_4^+/nss\text{-}Ca^{2+}$ were about 0.7 and 0.07 at Yongxing (Table 3), respectively. This may be because that $nss\text{-}SO_4^{2-}$ and $nss\text{-}Ca^{2+}$ were the major components from the continent, and demonstrated the presence of $CaSO_4$. There were large *R* among most ions (Table 2), suggesting that they existed in the following forms: NaCl, $CaCl_2$, $MgCl_2$, KCl, Na_2SO_4, $CaSO_4$, $MgSO_4$, K_2SO_4, $(NH_4)_2SO_4$, $NaNO_3$, $Ca(NO_3)_2$, $Mg(NO_3)_2$, KNO_3, and NH_4NO_3.

3.3.2 Principal component analysis and classical multidimensional scaling

Principal component analysis (PCA) was also used to explore the relationship among the aerosol ions at Yongxing Island (Fig. 9a). As seen in the figure, the first two components (PC1 and PC2) explained 96.0% of the variance in total and 84.5% and 11.5% individually. The first component captured the variance of Cl^-, Na^+, Ca^{2+}, K^+, Mg^{2+}, SO_4^{2-} and NO_3^-, indicating that they had common sources or chemical behaviors, as mentioned above. The angle between two ions and arrow lengths reflect their relationship and the contribution of different ions to the principal component. As shown in Fig. 9a, the samples from the cool season had a greater contribution to PC1 than in other seasons.

To better classify the ions, classical multidimensional scaling (CMDS) of the correlation coefficients based on Table 2 is plotted in Fig. 9b. As shown in that figure, in the same quadrant, they may have common sources or behaviors. For example, Na^+ and Cl^- in the same quadrant indicates that they possibly derived from sea salt. SO_4^{2-} and Ca^{2+} in the same quadrant implies that they likely existed in the form of $CaSO_4$ in the marine atmosphere. Although Mg^{2+} was alone in a quadrant, it was in the lower right quadrant with Na^+ and Cl^-, suggesting that they had a common source from sea salt, but different behaviors. Previous study reported that Na^+ may exist in super-micron size aerosol, and Mg^{2+} in sub-micron size aerosol (Moody et al., 2014). SO_4^{2-}, Ca^{2+}, K^+, Cl^- and Na^+ in the positive Dimension 1 indicates that they may exist in coarse particles. It was clear that NH_4^+ is widely separated from other ions, indicating that it was from a unique source.

3.3.3 Source identification and apportionment

Atmos. Chem. Phys. Discuss., doi:10.5194/acp-2016-885, 2016
Manuscript under review for journal Atmos. Chem. Phys.
Published: 7 November 2016

Based on the PMF model, five potential sources of atmospheric chemical components at Yongxing Island were identified: sea salt, crust, biomass burning, fossil fuel combustion, and marine biogenic. Table 3 summarizes source apportionment of the relative contributions of each identified source to the TSP and major ions. These sources have average contributions of 26% for sea salt and 53% for crust to TSP, and < 10% for others.

The first source, sea salt, generally has strong marine elements, such as Na^+ and Cl^-. They contributed 74% (Na^+) and 82% (Cl^-) from sea salt at Yongxing Island (Table 3). Other significant sources were crust, biomass burning, fossil fuel combustion and marine biogenic, with contributions < 10% for Na^+ and Cl^-. According to data of rainwater at Yongxing Island, a part of Na^+ and Cl^- could be from crust and produced by burning (Xiao et al., 2016). Coal combustion and biomass burning also produce Na^+ and Cl^- (Liu et al., 2000; Tiwari et al., 2013; Zhang et al., 2015). Zhang et al. (2015) found that coal combustion was the most likely dominant source of Cl^- in Beijing. The mole equivalent Cl^-/Na^+ ratios were larger in the cool season than in the transition and warm seasons at Yongxing, indicating that the crust, fossil combustion, and biofuel and biomass burning affected Na^+ and Cl^- concentrations over the Northwest Pacific (Figs. 8 and S2). As shown in Table 2, there were strong relationships between Na^+ (Cl^-) and SO_4^{2-} (Ca^{2+}, K^+), further proving that crust, fossil combustion and biomass burning can generate Na^+ and Cl^-. Moreover, NaCl can react with acids such as H_2SO_4, HNO_3 and $H_2C_2O_4$, altering Na^+ and Cl^- concentrations in the marine atmosphere and producing secondary chlorine-containing salt (Boreddy and Kawamura, 2015). Sea salt provided K^+, Mg^{2+} and SO_4^{2-}, constituting 42%, 63% and 31%, respectively. The results are consistent with other studies (Boreddy and Kawamura, 2015)

The second source, crust, has a substantial crustal element Ca^{2+}, which is a tracer of crust (Suzuki and Tsunogai, 1988; Xiao et al., 2013; Xiao and Liu, 2004). Absolutely, Ca^{2+} mainly came from the crust, which had a contribution of 50% (Table 3). A strong relationship between TSP and Ca^{2+} observed at Yongxing Island (R=0.92, p<0.01, Table 1) indicated that crust had a large contribution to TSP (53%; Table 3). Biomass burning and fossil combustion also had contributions (9% and 18%, respectively) to Ca^{2+}. $CaSO_4$ and sulfate containing both K and Ca have been observed in smoke and have been reported to originate from biomass burning (Allen and Miguel, 1995; Li et al., 2003). This implies that Asian biomass and biofuel burning increased Ca^{2+} concentrations of aerosols in the marine atmosphere. Studies have found that atmospheric Ca^{2+} also derives from fossil fuel combustion (Hutton and Symon, 1986). Some Ca^{2+} may be affected by local coral (Suzuki and Tsunogai, 1988; Xiao et al., 2016). There is a large percentage of live coral cover (Huang et al., 2006). Large corals have been dying with rapid development of the Xisha islands (including Yongxing), which have generated large amounts of $CaCO_3$ and become a source of Ca^{2+} in marine atmospheric aerosols (Xiao et al., 2014; Xiao et al., 2016).

Atmos. Chem. Phys. Discuss., doi:10.5194/acp-2016-885, 2016
Manuscript under review for journal Atmos. Chem. Phys.
Published: 7 November 2016

Atmospheric Chemistry and Physics Discussions

The third source, biomass burning, is characterized by substantial K^+, which is an effective tracer of biomass and biofuel burning aerosols (Zhang et al., 2015), with a contribution of 41% from such burning at Yongxing Island. K^+ salts and organic particles are the dominant species in smoke, with more KCl in young smoke, and K_2SO_4 and KNO_3 in aged smoke from biomass burning (Li et al., 2003). As shown in Figs. 8 and S2, biomass burning was more frequent in the cool season than in the warm and transition seasons over the Northwest Pacific, yielding ratios of K^+/Na^+ (neq/L) that were larger in the cool season (Table 2). Another main source for K^+ was sea salt, with a contribution of 42% (Table 3). In addition, biomass burning produces SO_2 and NO_x (Streets et al., 2003; Xiao et al., 2015; Zhang et al., 2015); they accounted for 7% of SO_4^{2-} and 1% of NO_3^-.

The fourth source is fossil fuel (especially coal) combustion, which releases large amounts of SO_2, NO_x and NH_3 (Xiao et al., 2012b; Xiao et al., 2014; Pan et al., 2016). Accordingly, fossil combustion contributed 22%, 56% and 26% to SO_4^{2-}, NO_3^- and NH_4^+ at Yongxing Island, respectively. SO_4^{2-} and NO_3^- emissions from fossil combustion may originate from Northern Asia in the cool season (Lawrence and Lelieveld, 2010; Xiao et al., 2015). In Chinese coastal provinces, emission intensities of SO_2 and NO_x were about 10 and 15 tons/km^2, respectively, much higher than other Chinese provinces (China Environment Statistical Yearbook, 2014). These results indicate that human activities clearly affected marine atmospheric chemical compositions.

The fifth source is marine biogenic, which released NO_x, NH_3 and DMS (Altieri et al., 2014; Jickells et al., 2003; Boreddy and Kawamura, 2015; Phinney et al., 2006), with respective contributions of 19% to NO_3^-, 69% to NH_4^+, and 38% to SO_4^{2-} at Yongxing Island (Table 3). Substantial NH_x may be released from degraded organic nitrogen-containing compounds and excretion from zooplankton in the ocean (Norman and Leck, 2005). The contribution of marine biogenic sources to NH_4^+ was much larger at Yongxing than at global marine atmospheric NH_x sources in the review of Duce et al. (2008), which showed 87.5% from anthropogenic sources. However, Altieri et al. (2014) found that the anthropogenic contribution was < 87.5% at Bermuda, an island in the North Atlantic Ocean (Fig. 5). DMS is the most abundant marine biogenic volatile sulfur emitted from the ocean surface to atmosphere, and can be oxidized to SO_4^{2-} in the marine atmosphere (Phinney et al., 2006). Yang et al. (2015) reported that biogenic SO_4^{2-} from the Bohai and northern Yellow seas near China was 0.114–0.551 μg/m^3, with an average of 0.247 μg/m^3, accounting for 1.4% of nss-SO_4^{2-}. Biogenic SO_4^{2-} in the northern SCS was ~1.2 and 0.6 μg/m^3 in summer and winter, respectively (Zhang et al., 2007), constituting ~8% and 12% of nss-SO_4^{2-}. However, large ratios of biogenic SO_4^{2-} to nss-SO_4^{2-} were observed at the remote Pacific islands of Oahu and Midway, at 55% and 70% (Arimoto et al., 1996), being consistent with our results. Thus, natural sources had large contributions to marine atmospheric aerosols over the Northwest Pacific.

Atmos. Chem. Phys. Discuss., doi:10.5194/acp-2016-885, 2016
Manuscript under review for journal Atmos. Chem. Phys.
Published: 7 November 2016

Atmospheric Chemistry and Physics Discussions

3.4 Regional sources deduced from trajectory and CWT analyses

Air masses at Yongxing Island had obvious unique and seasonal variations, from northeast of the island in the cool season, southwest in the warm season, and southeast in the transition season (Fig. 10). This reveals that aerosol or chemical compositions at the island originated from different regions in different seasons (Figs. 1, 8, 10 and S2). CWTs were plotted for TSP and major ions (Fig. 10) to explore likely regional sources and transport pathways for the island. A major discovery was that air masses with high TSP concentrations were from China coastal regions bordering the Yellow and East China Seas and northern South China (Fig. 10). This is consistent with the seasonal variations of TSP concentrations in Fig. 6. The average aerosol optical thickness (AOT) over the Northwest Pacific (Fig. 1) confirmed this result. A relatively large average AOT was found over the northern SCS and East China Sea in the cool season, and Karimata Strait in the warm season (Fig. 1). But there was a relatively low average AOT over the entire SCS in the transition season (Fig. 1).

CWTs for Ca^{2+} had a similar trend as that of TSP, larger in the cool season and lower in the warm season, indicating that dust from Northeast Asia influenced aerosol chemistry in the remote marine atmosphere (Figs. 1, 10 and S2). Although the CWT for Mg^{2+} was also larger in the cool season and lower in the warm season, air masses with relatively high concentrations of Mg^{2+} originated offshore of China (Fig. 10). This indicates that Mg^{2+} was mainly from sea salt, consistent with the PMF results (Table 3).

CWTs for K^+, SO_4^{2-}, and NO_3^- concentrations showed considerable seasonal variations, higher in the cool season and lower in the warm and transition seasons (Fig. 10). As with TSP and Ca^{2+}, air masses from China coastal regions had high SO_4^{2-} and NO_3^- concentrations in the cool season (Fig. 10), owing to rapid economic development and great coal demand in the country, especially in its coastal regions (Lawrence and Lelieveld, 2010). However, the three ions may have different sources; K^+ was mainly derived from biomass and biofuel burning in Northeast Asia (Fig. 8; Atwood et al., 2013; Streets et al., 2003), whereas NO_3^- and SO_4^{2-} were mainly from fossil fuel combustion in that region (Table 3; Xiao et al., 2014 and 2015a; Lawrence and Lelieveld, 2010). Figure S2 also shows that SO_4^{2-} from central and eastern China reached coastal regions in the cool season. According to data from the China Environment Statistical Yearbook (2014), average SO_2, NO_x, and soot and dust emissions from Chinese coastal regions (Liaoning, Hebei, Shandong, Jiangsu, Zhejiang, Fujian and Guangdong provinces, and the cities of Shanghai, Beijing and Tianjin) exceeded 10, 15 and 5 tons/km^2, respectively, much greater than other provinces or cities in the country. In addition, higher concentrations of SO_2 and NO_x in Northeast Asia than South Asia (Lawrence and Lelieveld, 2010) indicate that the marine atmospheric aerosol chemical compositions were

Atmos. Chem. Phys. Discuss., doi:10.5194/acp-2016-885, 2016
Manuscript under review for journal Atmos. Chem. Phys.
Published: 7 November 2016

Atmospheric Chemistry and Physics Discussions

influenced by Northeast Asia, especially China coastal regions in the cool season. Rapidly growing economies and high population densities in these regions (Kim et al., 2014) release pollutants that are transported to the Northwest Pacific. Biogenic SO_4^{2-} from the Chinese seas may affect the atmospheric aerosol chemical compositions.

As mentioned above, in Table 3, NH_4^+ may largely come from marine biogenic sources, and air masses with high NH_4^+ concentrations were from remote open oceans such as the southeastern and northeastern SCS (Fig. 10). This suggests that it is feasible for the ocean to be a NH_4^+ source. Globally, 87.5% of marine atmospheric NH_x is from human activities (Duce et al., 2008). However, there was little NH_x from such activities at Yongxing Island, consistent with Altieri et al. (2014). There were relatively higher NH_4^+ concentrations in the cool season and lower values in the warm season at Yongxing Island (Fig. 6). The Northwest Pacific Ocean including the SCS has oligotrophic surface water and is a nitrogen-limited region (Chen et al., 2004; Kim et al., 2014; Wu et al., 2001), with only a hundred nanomoles per liter of NH_4^+ in surface water (Lin, 2013). Thus, it is in some ways counterintuitive that marine atmospheric aerosol NH_4^+ at Yongxing Island is from marine sources. Altieri et al. (2014) suggested that the efficient kinetics of ammonia evasion from surface seawater causes NH_3 to accumulate in the marine atmosphere. NH_3 may be released from degraded organic nitrogen-containing compounds and excretion from zooplankton (Norman and Leck, 2005). Lin (2013) found average N_2 fixation rates in the SCS of 4.9 and 0.7 μmol $N/m^3/d$ in the cool season and warm seasons, respectively. He suggested that this seasonal variation may be caused by the intensity of the Kuroshio intrusion in the SCS and Fe supply from the atmosphere in the cool season, which enhances primary productivity. The unique temporal variations of N_2 fixation rates in the SCS are consistent with our CWT results. Moreover, as shown in Figs. 1 and S2, dust was transported to remote open oceans in the cool season, likely containing substantial Fe (Wu et al., 2001). Increased Fe would greatly increase productivity in these marine regions (Wu et al., 2001).

4 Conclusions

Chemical compositions of 1-year aerosols at Yongxing Island were investigated to help better understanding of their chemical characteristics, sources, and transport pathways over the SCS. Sea salt (Na^+ and Cl^-) had the greatest contribution to total major inorganic ions in aerosols at the island, followed by SO_4^{2-}, Ca^{2+}, NO_3^-, Mg^{2+}, K^+ and NH_4^+. The concentrations of TSP and all major inorganic ions showed seasonal variations, higher in the cool season and lower in the warm season, which was influenced by meteorological parameters (e.g., wind speed, temperature, relative humidity and rainfall) and air masses. Using PMF and CWT models, fire spot and AOT, we found that Na^+, Cl^-, and Mg^{2+} were mainly derived from sea salt, Ca^{2+} from soil dust, K^+ from biomass burning,

and NO_3^- from fossil fuel combustion (especially coal combustion in the Northern Asia). SO_4^{2-} was from marine biogenic sources, sea salt, and fossil fuel combustion. Surprisingly, NH_4^+ was mainly from marine biogenic processes in the remote ocean. In summary, Asian dust, biomass burning and fossil fuel combustion seriously affected marine atmospheric aerosol chemical compositions over the Northwest Pacific.

Acknowledgements This work was supported by the National Natural Science Foundation of China (Grant nos. 41425014, 41663003, and 41203015), Strategic Priority Research Program of the Chinese Academy of Sciences (Grant nos. XDA11030103 and XDA11020202), Doctoral Scientific Research Foundation of East China University of Technology (Grant no. DHBK2015327), and Scientific Research Foundation of East China University of Technology for Science and Technology Innovation Team (Grant no. DHKT2015101).

References

Allen, A.G. and Miguel, A.H.: Biomass burning in the Amazon: characterization of the ionic component of aerosols generated from flaming and smoldering rainforest and savannah, Environmental Science & Technology, 29(2), 486-93, 1995.

Altieri, K.E., Hastings, M.G., Peters, A.J., Oleynik, S. and Sigman, D.M.: Isotopic evidence for a marine ammonium source in rainwater at Bermuda, Global Biogeochemical Cycles, 28(10), 1066 – 1080, 2014.

Arakaki, T., Azechi, S., Somada, Y., Ijyu, M., Nakaema, F., Hitomi, Y., Handa, D., Oshiro, Y., Miyagi, Y. and Ai, T.: Spatial and temporal variations of chemicals in the TSP aerosols simultaneously collected at three islands in Okinawa, Japan, Atmospheric Environment, 97, 479-485, 2014.

Arimoto, R., Duce, R.A., Savoie, D.L., Prospero, J.M, Talbot, R., Cullen, J.D., Tomza, U., Lewis, N.F. and Ray, B.J.: Relationships among aerosol constitutes from Asia and the North Pacific during PEM-West A, Journal of Geophysical Research, 101, 2011-2023, 1996.

Atwood, S.A., Reid, J.S., Kreidenweis, S.M., Cliff, S.S., Zhao, Y., Lin, N.H., Tsay, S.C., Chu, Y.C. and Westphal, D.L.: Size resolved measurements of springtime aerosol particles over the northern South China Sea, Atmospheric Environment, 78(676), 134-143, 2013.

Balasubramanian, R., Karthikeyan, S., Potter, J., Wurl, O. and Durville, C.: Chemical characterization of aerosols in the equatorial atmosphere over the Indian Ocean, Atmospheric Environment, 78(3), 268-276, 2013.

Boreddy, S. and Kawamura, K.: A 12-year observation of water-soluble ions in TSP aerosols collected at a remote marine location in the western North Pacific: an outflow region of Asian dust, Atmospheric chemistry and physics, 15(11), 6437-6453, 2015.

Carrillo, J.H., Hastings, M.G., Sigman, D.M. and Huebert, B.J.: Atmospheric deposition of inorganic and organic nitrogen and base cations in Hawaii, Global Biogeochemical Cycles, 16(4), doi: 10.1029/2002GB001892, 2002

Chen, Y.L., Cheng, H.Y., Karl, D.M. and Takahashi, M.: Nitrogen modulates phytoplankton growth in spring in the South China Sea, Continental Shelf Research, 24, 527-541, 2004.

Cheng, Z.L., Lam, K.S., Chan, L.Y., Wang, T. and Cheng, K.K.: Chemical characteristics of aerosols at coastal station in Hong Kong. I. Seasonal variation of major ions, halogens and mineral dusts between 1995 and 1996, Atmospheric Environment, 34(17), 2771-2783, 2000.

Claeys, M., Wang, W., Vermeylen, R., Kourtchev, I., Chi, X., Farhat, Y., Surratt, J.D., Gómez-González, Y., Sciare, J. and Maenhaut, W.: Chemical characterisation of marine aerosol at Amsterdam Island during the austral summer of 2006–2007, Aerosol Science, 41, 13-22, 2010.

Cui, D.Y., Wang, J.T., Tan, L.J. and Dong, Z.Y.: Impact of atmospheric wet deposition on phytoplankton community structure in the South China Sea, Estuarine Coastal & Shelf Science, 173, 1 – 8, 2016.

Deng, C., Zhuang, G., Huang, K., Li, J., Zhang, R., Wang, Q., Liu, T., Sun, Y., Guo, Z. and Fu, J.S.: Chemical characterization of aerosols at the summit of Mountain Tai in Central East China, Atmospheric Chemistry & Physics, 11(14), 7319-7332, 2010.

Duan, F.K., He, K.B., Ma, Y.L., Yang, F.M., Yu, X.C., Cadle, S.H., Chan, T. and Mulawa, P.A.: Concentration and chemical characteristics of $PM_{2.5}$ in Beijing, China: 2001 – 2002, Science of the Total Environment, 355(1-3), 264-75, 2006.

Duce, R.A., Laroche, J., Altieri, K., Arrigo, K.R., Baker, A.R., Capone, D.G., Cornell, S., Dentener, F., Galloway, J. and Ganeshram, R.S.: Impacts of atmospheric anthropogenic nitrogen on the open ocean, Science, 320(5878), 893-7, 2008.

Ebert, M., Weinbruch, S., Hoffmann, P. and Ortner, H.M.: Chemical characterization of North Sea aerosol particles, Journal of Aerosol Science, 31(31), 613-632, 2000.

Fang, Y.T., Koba, K., Wang, X.M., Wen, D.Z., Li, J., Takebayashi, Y., Liu, X.Y. and Yoh, M.: Anthropogenic imprints on nitrogen and oxygen isotopic composition of precipitation nitrate in a nitrogen-polluted city in southern China, Atmospheric Chemistry and Physics, 11(3), 1313-1325, 2011.

Han, J.S., Moon, K.J., Lee, S.J., Kim, Y.J., Ryu, S.Y., Cliff, S.S. and Yi, S.M.: Size-resolved source apportionment of ambient particles by positive matrix factorization at Gosan background site in East Asia, Atmospheric Chemistry & Physics, 5(4), 211-223, 2006.

Hien, P.D., Bac, V.T. and Thinh, N.: PMF receptor modelling of fine and coarse PM_{10} in air masses governing monsoon conditions in Hanoi, northern Vietnam, Atmospheric Environment, 38(2), 189-201, 2004.

Hsu, S.C., Liu, S.C., Kao, S.J., Jeng, W.L., Huang, Y.T., Tseng, C.M., Tsai, F., Tu, J.Y. and Yang, Y.: Water-soluble species in the marine aerosol from the northern South China Sea: High chloride depletion related to air pollution, Journal of Geophysical Research Atmospheres, 112(D19), 216-229, 2007.

Huang, H., Lian, J., Huang, X., Huang, L., Zou, R. and Wang, D.: Coral cover as a proxy of disturbance: a case study of the biodiversity of the hermatypic corals in Yongxing Island, Xisha Islands in the South China Sea, Chinese Science Bulletin, 51(2), 129-135, 2006.

Hutton, M. and Symon, C.: The quantities of cadmium, lead, mercury and arsenic entering the U.K. environment from human activities, Science of the Total Environment, 57(3), 129-50, 1986.

Jia, G. and Chen, F.: Monthly variations in nitrogen isotopes of ammonium and nitrate in wet deposition at Guangzhou, south China, Atmospheric Environment, 44(19), 2309-2315, 2010.

Jickells, T.D., Kelly, S.D., Baker, A.R., Biswas, K., Dennis, P.F., Spokes, L.J., Witt, M. and Yeatman, S.G.: Isotopic evidence for a marine ammonia source, Geophysical Research Letters, 30(7), 359-376, 2003.

Jung, J., Furutani, H. and Uematsu, M.: Atmospheric inorganic nitrogen in marine aerosol and precipitation and its deposition to the North and South Pacific Oceans, Journal of Atmospheric Chemistry, 68(2), 157-181, 2012.

Keene, W.C., Moody, J.L., Galloway, J.N., Prospero, J.M., Cooper, O.R., Eckhardt, S. and Maben, J.R.: Long-term trends in aerosol and precipitation composition over the western North Atlantic Ocean at Bermuda, Atmospheric Chemistry & Physics, 29(14), 292-303, 2005.

Kim, T.W., Lee, K., Duce, R. and Liss, P.: Impact of atmospheric nitrogen deposition on phytoplankton productivity in the South China Sea, Geophysical Research Letters, 41(9), 3156-3162, 2014.

Kolb, C.E. and Worsnop, D.R.: ChemInform Abstract: Chemistry and Composition of Atmospheric Aerosol Particles, Annual Review of Physical Chemistry, 44(63), 471-491, 2013.

Kumar, A., Sudheer, A.K. and Sarin, M.M.: Chemical characteristics of aerosols in MABL of Bay of Bengal and Arabian Sea during spring inter-monsoon: A comparative study, Journal of Earth System Science, 117(S1), 325-332, 2008.

Landing, W.M. and Paytan, A.: Marine chemistry special issue: Aerosol chemistry and impacts on the ocean, Marine Chemistry, 120(1), 1-3, 2010.

Lawrence, M.G. and Lelieveld, J.: Atmospheric pollutant outflow from southern Asia: a review, Atmospheric Chemistry & Physics, 10(22), 11017-11096, 2010.

Li, J., Pósfai, M., Hobbs, P.V. and Buseck, P.R.: Individual aerosol particles from biomass burning in southern Africa: 2, Compositions and aging of inorganic particles, Journal of Geophysical Research Atmospheres, 108(13), 347-362, 2003.

Lin, F.: Spatial and temporal variations of biological N_2 fixation rate and its controlling factors in the China marginal seas, Xiamen University, 2013.

Liu, X., Espen, P.V., Adams, F., Cafmeyer, J. and Maenhaut, W.: Biomass Burning in Southern Africa: Individual Particle Characterization of Atmospheric Aerosols and Savanna Fire Samples, Journal of Atmospheric Chemistry, 36(2), 135-155, 2000.

Liu, X., Zhang, Y., Han, W., Tang, A., Shen, J., Cui, Z., Vitousek, P., Erisman, J.W., Goulding, K. and Christie, P.: Enhanced nitrogen deposition over China, Nature, 494(7438), 459-62, 2013.

Liu, Y., Sun, L., Zhou, X., Luo, Y., Huang, W., Yang, C., Wang, Y. and Huang, T.: A 1400-year terrigenous dust record on a coral island in South China Sea, Scientific Reports, 4(20), 4994-4994, 2014.

Moody, J.L., Keene, W.C., Cooper, O.R., Voss, K.J., Aryal, R., Eckhardt, S., Holben, B., Maben, J.R., Izaguirre, A. and Galloway, J.N.: Flow climatology for physicochemical properties ofdichotomous aerosol over the western North Atlantic

Ocean at Bermuda, Atmospheric Chemistry and Physics, 14, 691-717, 2014.

Naga, Kavuri, Kakoli, Karar, Paul and Nagendra: TSP aerosol source apportionment in the urban region of the Indian steel city, Rourkela, Particuology, 20(3), 124-133, 2014.

Norman, M. and Leck, C.: Distribution of marine boundary layer ammonia over the Atlantic and Indian Oceans during the Aerosols99 cruise, Journal of Geophysical Research, doi:10.1029/2005JD005866, 2005.

Okuda, T., Tenmoku, M., Kato, J., Mori, J., Sato, T., Yokochi, R. and Tanaka, S.: Long-term observation of trace metal concentration in aerosols at a remote island, Rishiri, Japan by using inductively coupled plasma mass spectrometry equipped with laser ablation, Water, Air, and Soil Pollution, 174, 3-17, 2006.

Ooki, A., Uematsu, M. and Noriki, S.: Size-resolved sulfate and ammonium measurements in marine boundary layer over the North and South Pacific, Atmospheric Environment, 41(1), 81-91, 2007.

Ottley, C.J. and Harrison, R.M.: The spatial distribution and particle size of some inorganic nitrogen, sulphur and chlorine species over the North Sea, Atmospheric Environment. Part A. General Topics, 26(9), 1689-1699, 1992.

Pan, Y., Tian, S., Liu, D., Fang, Y., Zhu, X., Zhang, Q., Zheng, B., Michalshi, G., and Wang, Y.: Fossil fuel combustion-related emissions dominate atmospheric ammonia sources during severe haze episodes: Evidence from 15N-stable isotope in size-resolved aerosol ammonium, Environmental Science & Technology, DOI: 10.1021/acs.est.6b00634.

Phinney, L., Leaitch, W.R., Lohmann, U., Boudries, H., Worsnop, D.R., Jayne, J.T., Toom-Sauntry, D., Wadleigh, M., Sharma, S. and Shantz, N.: Characterization of the aerosol over the sub-arctic north east Pacific Ocean, Deep Sea Research Part II Topical Studies in Oceanography, 53(20 – 22), 2410-2433, 2006.

Price, C., Penner, J. and Prather, M.: NO_x from lightning: 1. Global distribution based on lightning physics, Journal of Geophysical Research Atmospheres, 102(D5), 5929-5942, 1997.

Schmale, J., Schneider, J., Nemitz, E., Tang, Y.S., Dragosits, U., Blackall, T.D., Trathan, P.N., Phillips, G.J., Sutton, M. and Braban, C.F.: Sub-Antarctic marine aerosol: dominant contributions from biogenic sources, Atmospheric Chemistry & Physics, 13(17), 8669-8694, 2013.

Streets, D.G., Yarber, K.F., Woo, J.H. and Carmichael, G.R.: Biomass burning in Asia: annual and seasonal estimates and atmospheric emissions, Global Biogeochem Cycles J, 17(4), 1759-1768, 2003.

Suzuki, T. and Tsunogai, S.: Origin of calcium in aerosols over the western north Pacific, Journal of Atmospheric Chemistry, 6(4), 363-374, 1988.

Tiwari, S., Pervez, S., Cinzia, P., Bisht, D.S., Kumar, A. and Chate, D.: Chemical characterization of atmospheric particulate matter in Delhi, India, part II: Source apportionment studies using PMF 3.0, Sustainable Environment Research, 23, 295-306, 2013.

Wang, L., Qi, J.H., Shi, J.H., Chen, X.J. and Gao, H.W.: Source apportionment of particulate pollutants in the atmosphere over the Northern Yellow Sea, Atmospheric Environment, 70(4), 425-434, 2013.

Wang, S.H., Hsu, N.C., Tsay, S.C., Lin, N.H., Sayer, A.M., Huang, S.J. and Lau, W.K.: Can Asian dust trigger phytoplankton

blooms in the oligotrophic northern South China Sea?, Geophysical Research Letters, 39(5), 2012.

Wang, S.H., Tsay, S.C., Lin, N.H., Chang, S.C., Li, C., Welton, E.J., Holben, B.N., Hsu, N.C., Lau, W.K.M. and Lolli, S.: Origin, transport, and vertical distribution of atmospheric pollutants over the northern South China Sea during the 7-SEAS/Dongsha Experiment, Atmospheric Environment, 78(3), 124 – 133, 2013.

Wang, S.H., Tsay, S.C., Lin, N.H., Hsu, N.C., Bell, S.W., Li, C., Ji, Q., Jeong, M.J., Hansell, R.A. and Welton, E.J.: First detailed observations of long-range transported dust over the northern South China Sea, Atmospheric Environment, 45(27), 4804-4808, 2011.

Wang, Y., Zhuang, G., Zhang, X., Huang, K., Xu, C., Tang, A., Chen, J. and An, Z.: The ion chemistry, seasonal cycle, and sources of $PM_{2.5}$ and TSP aerosol in Shanghai, Atmospheric Environment, 40(16), 2935-2952, 2006.

Wu, J., Boyle, E., Sunda, W. and Wen, L.S.: Soluble and Colloidal Iron in the Oligotrophic North Atlantic and North Pacific, Science, 293(5531), 847-9, 2001.

Xiao, H., Long, A., Xie, L., Xiao, H. and Liu, C.: Chemical characteristics of precipitation in South China Sea, Environmental Science, 35(2), 475-480, 2014 (Chinese with English Abstract).

Xiao, H., Xiao, H., Long, A. and Wang, Y.: Who controls the monthly variations of NH_4^+ nitrogen isotope composition in precipitation?, Atmospheric Environment, 54, 201-206, 2012a.

Xiao, H., Xiao, H., Long, A. and Wang, Y.: Nitrogen isotopic composition and source of nitrate in precipitation at Guiyang, Acta Scientiae Circumstantiae, 32(4), 940-945, 2012b (Chinese with English Abstract).

Xiao, H., Xiao, H., Long, A., Wang, Y. and Liu, C.: Chemical composition and source apportionment of rainwater at Guiyang, SW China, Journal of Atmospheric Chemistry, 70(3), 269-281, 2013.

Xiao, H., Xiao, H., Long, A., Wang, Y. and Liu, C.: Sources and meteorological factors that control seasonal variation of $\delta^{34}S$ values in rainwater, Atmospheric Research, 149, 154-165, 2014.

Xiao, H., Xiao, H., Zhang, Z., Wang, Y., Long, A. and Liu, C.: Chemical characteristics and source apportionment sources of precipitation in Yongxing Island, China Environmental Science, 36(11), 2016 (Chinese with English Abstract).

Xiao, H., Xie, L., Long, A., Ye, F., Pan, Y., Li, D., Long, Z., Chen, L., Xiao, H. and Liu, C.: Use of isotopic compositions of nitrate in TSP to identify sources and chemistry in South China Sea, Atmospheric Environment, 109, 70-78, 2015.

Xiao, H.Y. and Liu, C.Q.: Sources of nitrogen and sulfur in wet deposition at Guiyang, southwest China, Atmospheric Environment, 36(33), 5121-5130, 2002.

Xiao, H.Y. and Liu, C.Q.: Chemical characteristics of water-soluble components in TSP over Guiyang, SW China, 2003, Atmospheric Environment, 38(37), 6297-6306, 2004.

Yang, G., Zhang, S., Zhang, H., Yang, J. and Liu, C.: Distribution of biogenic sulfur in the Bohai Sea and northern Yellow Sea and its contribution to atmospheric sulfate aerosol in the late fall, Marine Chemistry, 169, 23-32, 2015.

Yu, L., Wang, G., Zhang, R., Zhang, L., Song, Y., Wu, B., Li, X., An, K. and Chu, J.: Characterization and Source Apportionment of $PM_{2.5}$ in an Urban Environment in Beijing, Aerosol & Air Quality Research, 13(2), 574-583, 2013.

Zhang, M., Chen, J.M., Wang, T., Cheng, T.T., Lin, L., Bhatia, R.S. and Havey, M.: Chemical characterization of aerosols over the Atlantic Ocean and the Pacific Ocean during two cruises in 2007 and 2008, Journal of Geophysical Research, 115, 1842-1851, 2010.

Zhang, N., Cao, J., Liu, S., Zhao, Z.Z., Xu, H. and Xiao, S.: Chemical composition and sources of $PM_{2.5}$ and TSP collected at Qinghai Lake during summertime, Atmospheric Research, 138(3), 213–222, 2014.

Zhang, R., Jing, J., Tao, J., Hsu, S.C., Wang, G., Cao, J., Lee, C.S.L., Zhu, L., Chen, Z. and Zhao, Y.: Chemical characterization and source apportionment of PM2.5 in Beijing: Seasonal perspective, Atmospheric Chemistry and Physics, 7053-7074, 2015.

Zhang, X., Zhuang, G., Guo, J., Yin, K. and Zhang, P.: Characterization of aerosol over the Northern South China Sea during two cruises in 2003, Atmospheric Environment, 41(36), 7821-7836, 2007.

Zhang, X.Y., Wang, Y.Q., Niu, T., Zhang, X.C., Gong, S.L., Zhang, Y.M. and Sun, J.Y.: Atmospheric aerosol compositions in China: spatial/temporal variability, chemical signature, regional haze distribution and comparisons with global aerosols, Atmospheric Chemistry and Physics, 12(2), 779-799, 2012.

Zhao, R., Han, B., Lu, B., Zhang, N., Zhu, L. and Bai, Z.: Element composition and source apportionment of atmospheric aerosols over the China Sea, Atmospheric Pollution Research, 6(2), 191-201, 2015.

Table Captions

Table 1 Correlation coefficients among major ions in aerosol and meteorological parameters.

Table 2 Mole equivalent ratios for major ionic species in aerosols at Yongxing Island (annual, cool, transition and warm seasons), together with seawater ratios for comparison.

Table 3 Relative contributions (%) for different major ions from six factors of TSP at Yongxing Island over the year, based on PMF model.

Figure Captions

Figure 1 Distribution of seasonal average aerosol optical thickness (AOT) at 550 nm (T550) over Northwest Pacific in cool, warm and transition seasons during sampling period. Monthly AOT products (from Moderate Resolution Imaging Spectrometer, MODIS) with 4-km resolution were downloaded from Globcolour (http://hermes.acri.fr/). The GlobColour project began in 2005 as an ESA Data User Element project to provide a continuous dataset of merged Level 3 Ocean Colour products.

Atmos. Chem. Phys. Discuss., doi:10.5194/acp-2016-885, 2016
Manuscript under review for journal Atmos. Chem. Phys.
Published: 7 November 2016

Atmospheric Chemistry and Physics Discussions

Figure 2 Three-hour temperature, relative humidity, wind speed and precipitation at Yongxing Island during sampling period (March 2014 through February 2015).

Figure 3 Annual average mass concentrations of aerosol chemical species at Yongxing Island. Box boundary indicates 25th and 75th percentile. Lines within the box show the mean. Whiskers above and below the box indicate 90th and 10th percentiles.

Figure 4 Mean contributions of each major ionic component to total ionic mass concentration of (a) Yongxing Island (YXI) annual, (b) YXI cool season, (c) YXI warm season, and (d) YXI transition season.

Figure 5 Comparisons of major ions in aerosol at Yongxing Island with global ocean. Data of Oki, Ogasawara and Hedo are from EANET (www.eanet.asia); those of Rishiri Island are from Okuda et al. (2006); those of Hawaii are from Carrillo et al. (2002); those of Bermuda are from Moody et al. (2014); those of Amsterdam Island are from Claeys et al. (2010); those of the Arabian Sea and Indian Ocean are from Kumar et al. (2008); those of Helgoland are from Ebert et al. (2000); those of the Mediterranean Sea, northern Atlantic-1 and 2, Pacific and southern Atlantic are from Zhang et al. (2010). Pentagrams represent sampling sites on islands; others represent cruises. N.A. indicates no data.

Figure 6 Seasonal variations of TSP mass concentration and associated species, including Na^+, Cl^-, SO_4^{2-}, Mg^{2+}, K^+, Ca^{2+}, NH_4^+, and NO_3^- at Yongxing Island (cool season: C; warm season: W; annual: A). Shown are the mean and standard deviation for each bar.

Figure 7 Comparison of aerosol chemical species between Yongxing Island and around the South China Sea (data from EANET).

Figure 8 Fire spot data from MODIS global fire mapping from March 2014 to February 2015 around South China Sea (https://firms.modaps.eosdis.nasa.gov/firemap/).

Figure 9 Plots of (a) principal component analysis (PCA) and (b) classical multidimensional scaling (CMDS) of correlation coefficients among major ions in aerosol samples.

Figure 10 Ten-day back trajectories of warm (black, June through September 2014), cool (blue, March and April 2014 and October 2014 through February 2015) seasons, and transition season (red, May 2014) at Yongxing Island. Additionally, CWT (concentration weighted trajectory) plots for daily weighted-average concentrations of TSP, Ca^{2+}, Mg^{2+}, K^+, SO_4^{2-}, NO_3^- and NH_4^+ at Yongxing Island.

Supporting Information

Figure S1. Plot from principal component analysis (PCA) for species and environmental variables.

Atmos. Chem. Phys. Discuss., doi:10.5194/acp-2016-885, 2016
Manuscript under review for journal Atmos. Chem. Phys.
Published: 7 November 2016

Atmospheric Chemistry and Physics Discussions

765 **Figure S2.** Modeled NAAPS total aerosol optical depth (AOD) for every month of March 2014 through February 2015, for total, sulfate, dust and smoke (data from http://www.nrlmry.navy.mil/aerosol/#aerosolobservations).

Atmos. Chem. Phys. Discuss., doi:10.5194/acp-2016-885, 2016
Manuscript under review for journal Atmos. Chem. Phys.
Published: 7 November 2016

Atmospheric Chemistry and Physics Discussions

767 **Table 1** Correlation coefficients among major ions in aerosol and meteorological parameters.

	TSP	Na^+	Cl^-	SO_4^{2-}	Ca^{2+}	Mg^{2+}	K^+	NH_4^+	NO_3^-	WS	T	RH	R
TSP	1	0.77**	0.92**	0.77**	0.92**	0.32**	0.75**	-0.05	0.52**	0.36**	-0.47**	-0.44**	-0.20
Na^+		1	0.91**	0.69**	0.72**	0.57**	0.78**	-0.03	0.48**	0.44**	-0.51**	-0.46**	-0.27*
Cl^-			1	0.71**	0.83**	0.49**	0.77**	-0.04	0.45**	0.43**	-0.37**	-0.36**	-0.19
SO_4^{2-}				1	0.86**	0.56**	0.85**	0.26*	0.87**	0.04	-0.56**	-0.58**	-0.29*
Ca^{2+}					1	0.36**	0.81**	-0.03	0.69**	0.24	-0.51**	-0.53**	-0.27*
Mg^{2+}						1	0.63**	0.45**	0.59**	0.04	-0.12	-0.08	-0.18
K^+							1	-0.18	0.72**	0.15	-0.51**	-0.45**	-0.27*
NH_4^+								1	0.36**	-0.13	-0.18	0.11	-0.18
NO_3^-									1	-0.05	-0.50**	-0.50**	-0.31**

768 **Correlation significant at 0.01 level (2-tailed), * significant at 0.05 level (2-tailed). WS: wind speed (m/s); T: temperature (°C); RH: relative humidity (%); R: rainfall (mm/h)

Atmos. Chem. Phys. Discuss., doi:10.5194/acp-2016-885, 2016
Manuscript under review for journal Atmos. Chem. Phys.
Published: 7 November 2016

Atmospheric Chemistry and Physics Discussions

769 **Table 2** Mole equivalent ratios for major ionic species in aerosols at Yongxing Island (annual,
770 cool, transition and warm seasons), together with seawater ratios for comparison.

	Yongxing Island				Seawater[a]
	annual	cool	transition	warm	
Cl^-/Na^+	1.25	1.31	1.06	1.12	1.17
Mg^{2+}/Na^+	0.21	0.21	0.19	0.23	0.22
K^+/Na^+	0.048	0.051	0.040	0.042	0.021
Ca^{2+}/Na^+	0.62	0.64	0.83	0.47	0.044
SO_4^{2-}/Na^+	0.66	0.71	0.73	0.51	0.12
nss-SO_4^{2-}/Na^+	0.54	0.58	0.61	0.39	-
NO_3^-/Na^+	0.18	0.18	0.22	0.16	-
NH_4^+/Na^+	0.022	0.021	0.044	0.016	-
NO_3^-/nss-SO_4^{2-}	0.34	0.32	0.36	0.41	-
NH_4^+/nss-Ca^{2+}	0.038	0.035	0.056	0.038	-

771 [a]Seawater ratios from Keene et al. (1986).

Atmos. Chem. Phys. Discuss., doi:10.5194/acp-2016-885, 2016
Manuscript under review for journal Atmos. Chem. Phys.
Published: 7 November 2016

Atmospheric Chemistry and Physics Discussions

772 **Table 3** Relative contributions (%) for different major ions from potential five sources of TSP
773 at Yongxing Island over the year, based on PMF model.

Source	TSP	Na^+	Cl^-	K^+	Ca^{2+}	Mg^{2+}	SO_4^{2-}	NO_3^-	NH_4^+
Sea salt	26	74	82	42	8	63	31	14	1
Crust	53	1	10	7	50	2	2	10	3
Biomass burning	7	5		41	9	16	7	1	
Fossil fuel combustion	7		4		18		22	56	26
Marine biogenic sources	7	20	4	10	15	18	38	19	69

774

Atmos. Chem. Phys. Discuss., doi:10.5194/acp-2016-885, 2016
Manuscript under review for journal Atmos. Chem. Phys.
Published: 7 November 2016

Atmospheric Chemistry and Physics Discussions

775 **Figure 1** Distribution of seasonal average aerosol optical thickness (AOT) at 550 nm (T550) over Northwest Pacific in cool, warm and transition seasons during
776 sampling period. Monthly AOT products (from Moderate Resolution Imaging Spectrometer, MODIS) with 4-km resolution were downloaded from Globcolour
777 (http://hermes.acri.fr/). The GlobColour project began in 2005 as an ESA Data User Element project to provide a continuous dataset of merged Level 3 Ocean
778 Colour products.

779 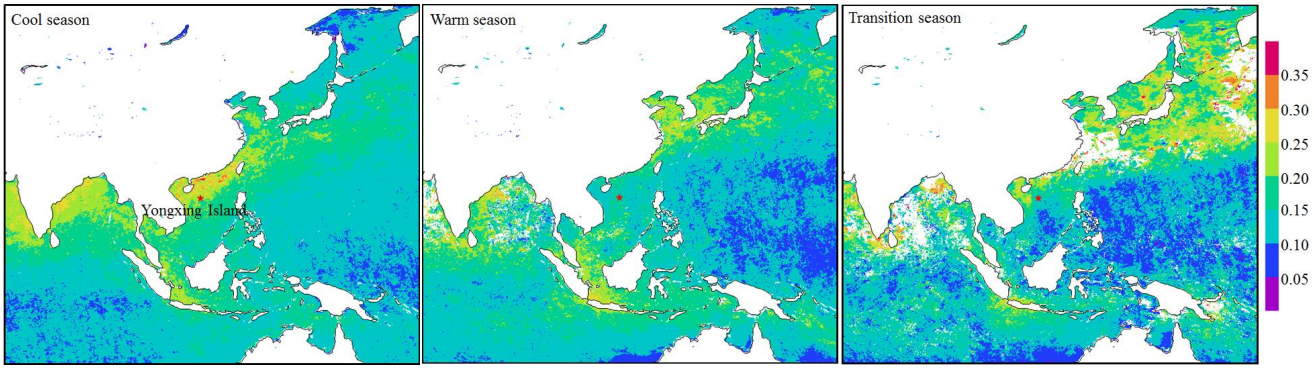

Atmos. Chem. Phys. Discuss., doi:10.5194/acp-2016-885, 2016
Manuscript under review for journal Atmos. Chem. Phys.
Published: 7 November 2016

Atmospheric Chemistry and Physics Discussions

780 **Figure 2** Three-hour temperature, relative humidity, wind speed and precipitation at Yongxing
781 Island during sampling period (March 2014 through February 2015).

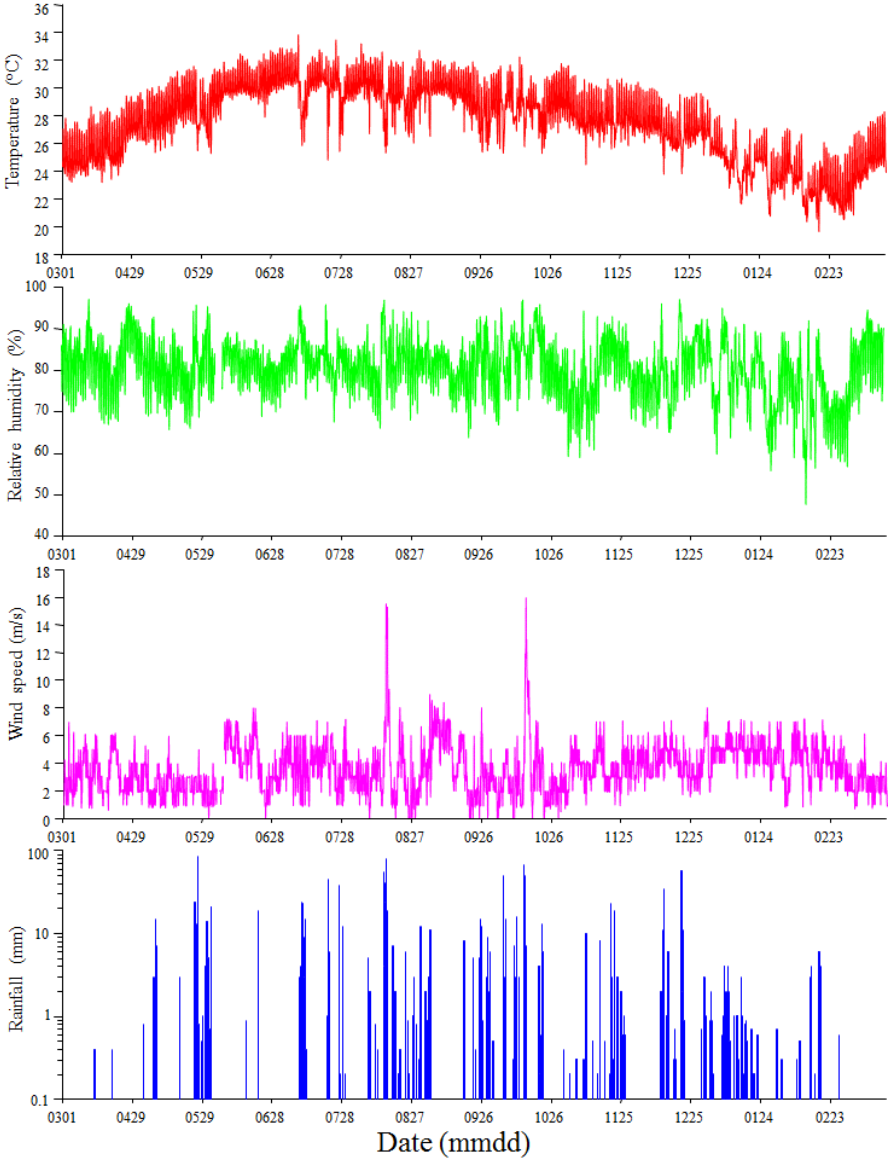

782

Atmos. Chem. Phys. Discuss., doi:10.5194/acp-2016-885, 2016
Manuscript under review for journal Atmos. Chem. Phys.
Published: 7 November 2016

Atmospheric Chemistry and Physics Discussions

783 **Figure 3** Annual average mass concentrations of aerosol chemical species at Yongxing Island.
784 Box boundary indicates 25th and 75th percentile. Lines within the box show the mean. Whiskers
785 above and below the box indicate 90th and 10th percentiles.

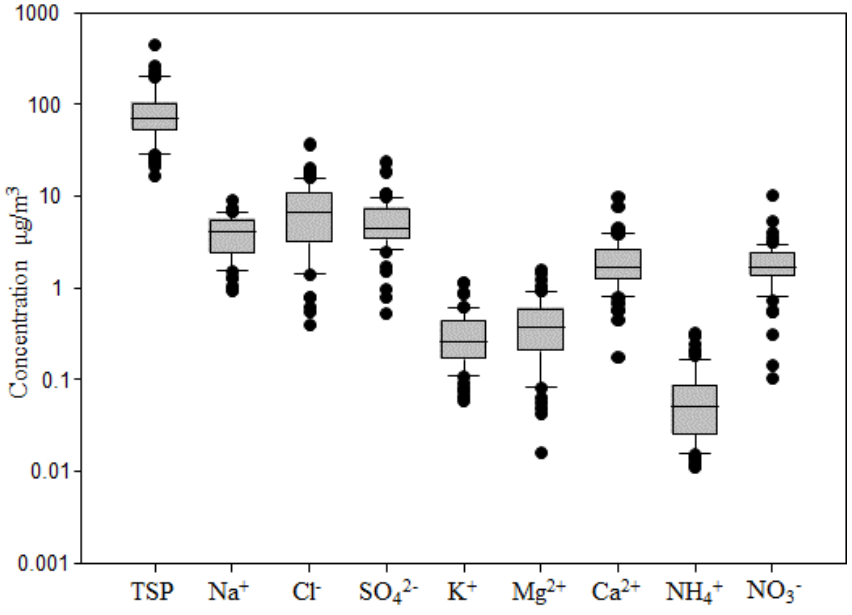

786

Atmos. Chem. Phys. Discuss., doi:10.5194/acp-2016-885, 2016
Manuscript under review for journal Atmos. Chem. Phys.
Published: 7 November 2016

Atmospheric Chemistry and Physics Discussions

787 **Figure 4** Mean contributions of each major ionic component to total ionic mass concentration
788 of (a) Yongxing Island (YXI) annual, (b) YXI cool season, (c) YXI warm season, and (d) YXI
789 transition season.

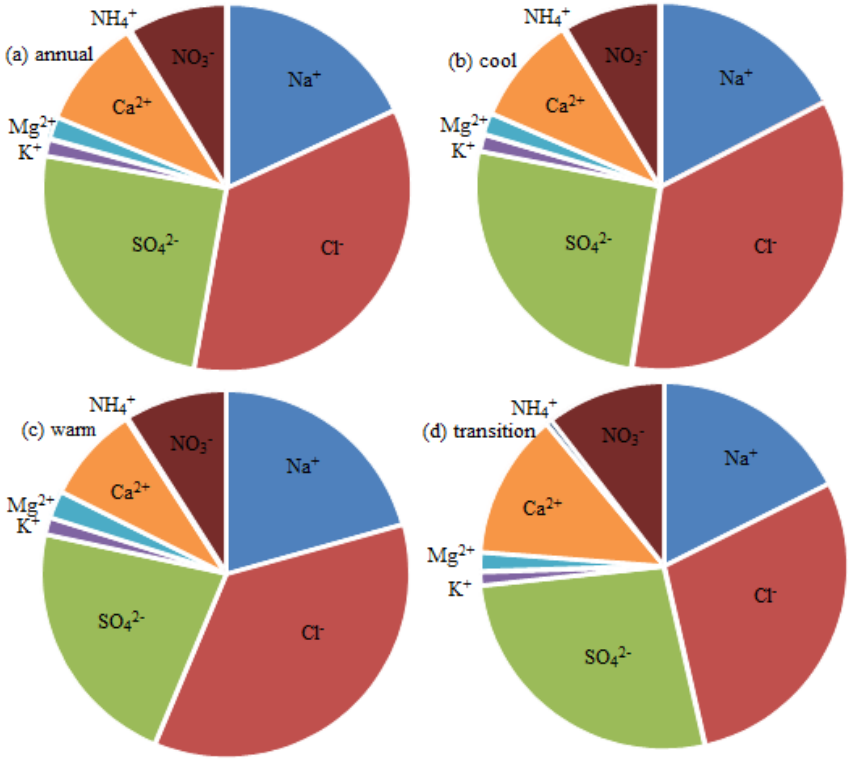

790

Atmos. Chem. Phys. Discuss., doi:10.5194/acp-2016-885, 2016
Manuscript under review for journal Atmos. Chem. Phys.
Published: 7 November 2016

Atmospheric Chemistry and Physics Discussions

Figure 5 Comparisons of major ions in aerosol at Yongxing Island with global ocean. Data of Oki, Ogasawara and Hedo are from EANET (www.eanet.asia); those of Rishiri Island are from Okuda et al. (2006); those of Hawaii are from Carrillo et al. (2002); those of Bermuda are from Moody et al. (2014); those of Amsterdam Island are from Claeys et al. (2010); those of the Arabian Sea and Indian Ocean are from Kumar et al. (2008); those of Helgoland are from Ebert et al. (2000); those of the Mediterranean Sea, northern Atlantic-1 and 2, Pacific and southern Atlantic are from Zhang et al. (2010). Pentagrams represent sampling sites on islands; others represent cruises. N.A. indicates no data.

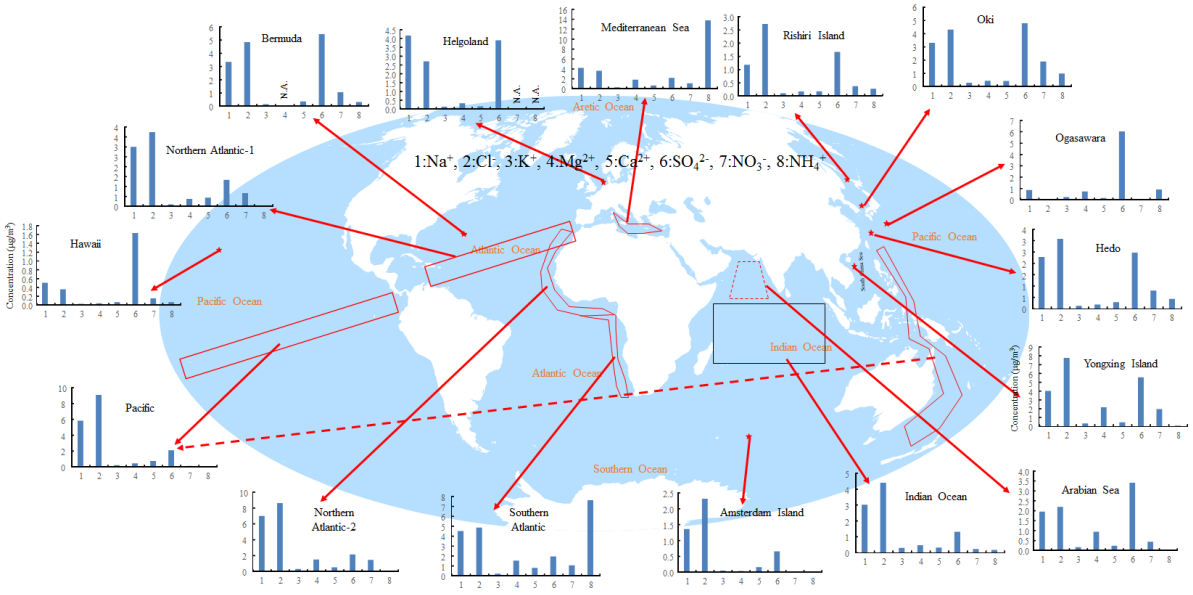

Atmos. Chem. Phys. Discuss., doi:10.5194/acp-2016-885, 2016
Manuscript under review for journal Atmos. Chem. Phys.
Published: 7 November 2016

Atmospheric Chemistry and Physics Discussions

797 **Figure 6** Seasonal variations of TSP mass concentration and associated species, including Na^+, Cl^-, SO_4^{2-}, Mg^{2+}, K^+, Ca^{2+}, NH_4^+, and NO_3^- at Yongxing Island
798 (cool season: C; warm season: W; annual: A). Shown are the mean and standard deviation for each bar.

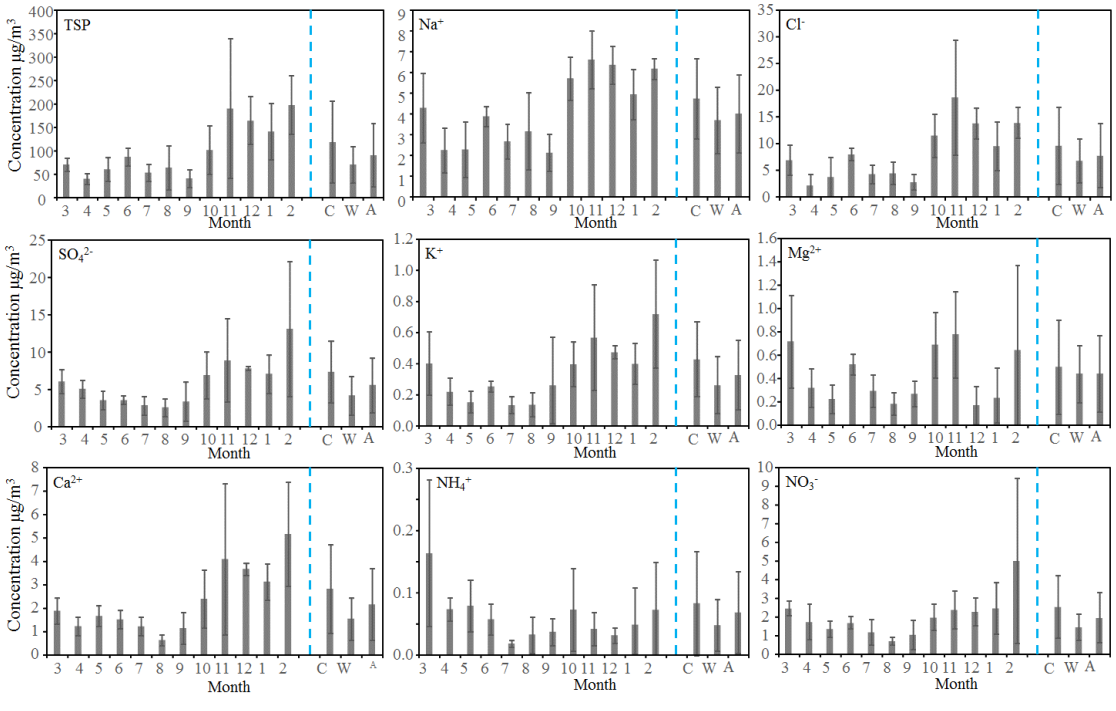

799

Atmos. Chem. Phys. Discuss., doi:10.5194/acp-2016-885, 2016
Manuscript under review for journal Atmos. Chem. Phys.
Published: 7 November 2016

Atmospheric Chemistry and Physics Discussions

800 **Figure 7** Comparison of aerosol chemical species between Yongxing Island and around the South China Sea (data from EANET).

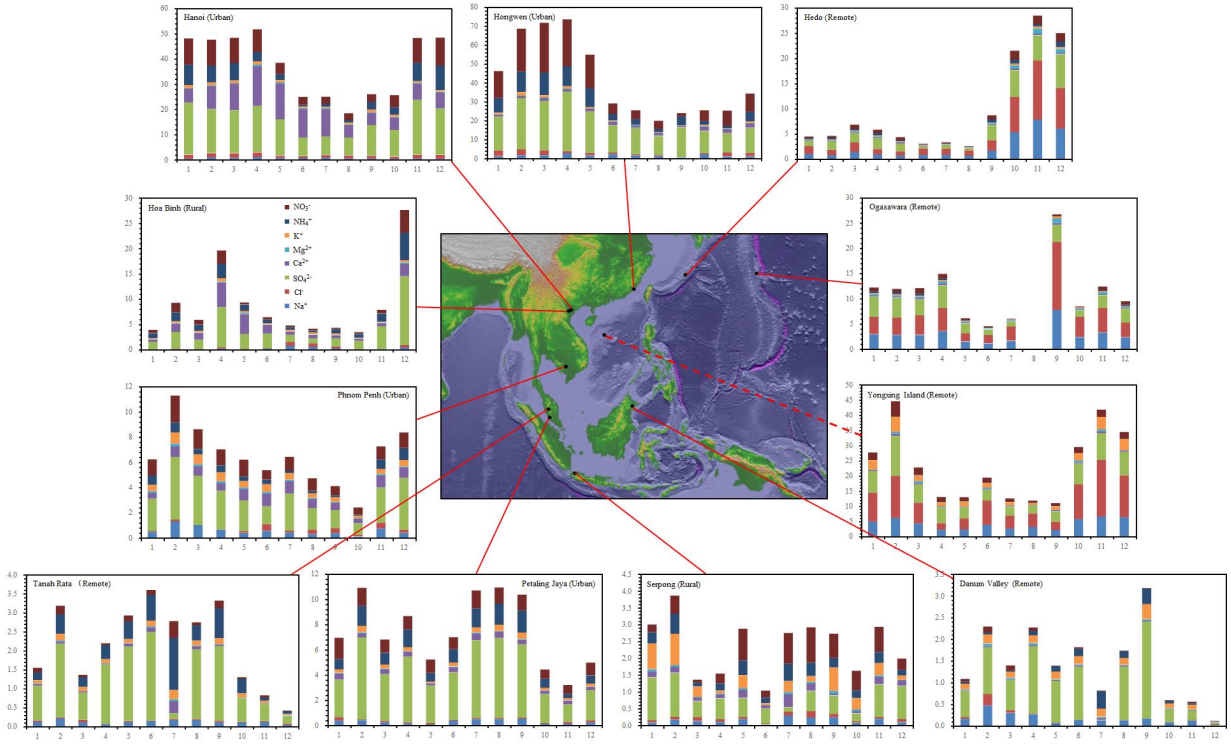

801

Atmos. Chem. Phys. Discuss., doi:10.5194/acp-2016-885, 2016
Manuscript under review for journal Atmos. Chem. Phys.
Published: 7 November 2016

Atmospheric Chemistry and Physics Discussions

802 **Figure 8** Fire spot data from MODIS global fire mapping from March 2014 to February 2015 around South China Sea
803 (https://firms.modaps.eosdis.nasa.gov/firemap/).

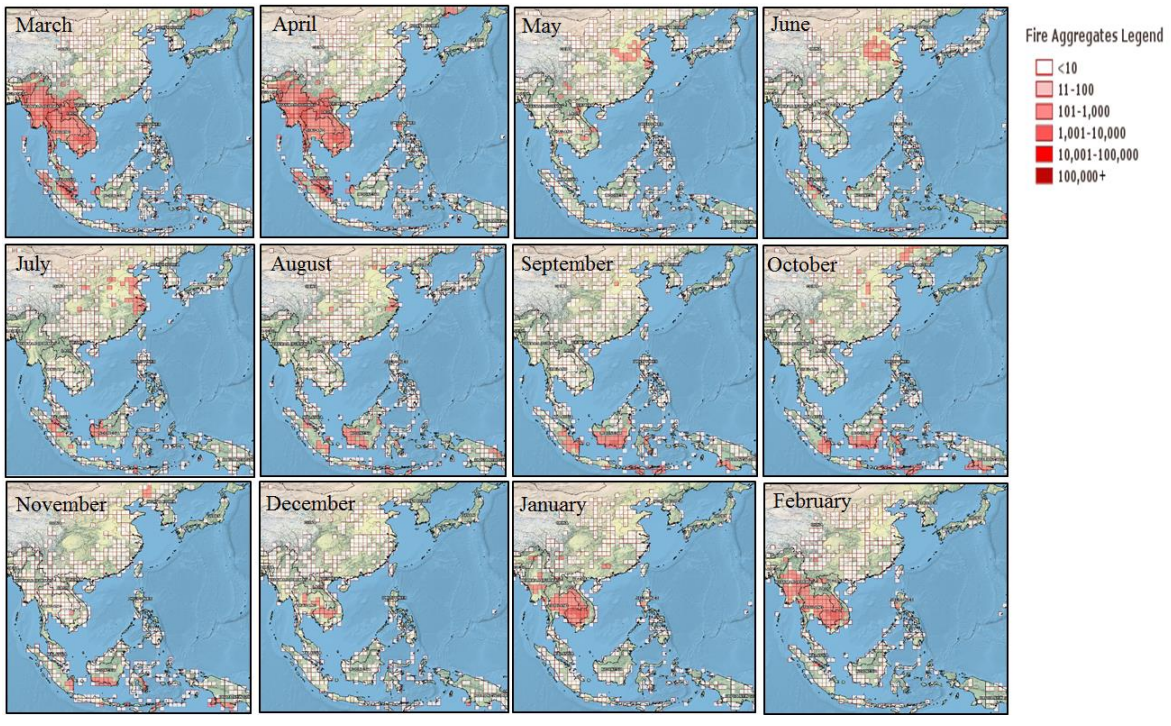

804

Atmos. Chem. Phys. Discuss., doi:10.5194/acp-2016-885, 2016
Manuscript under review for journal Atmos. Chem. Phys.
Published: 7 November 2016

Atmospheric Chemistry and Physics Discussions

805 **Figure 9** Plots of (a) principal component analysis (PCA) and (b) classical multidimensional scaling (CMDS) of correlation coefficients among major ions in
806 aerosol samples.

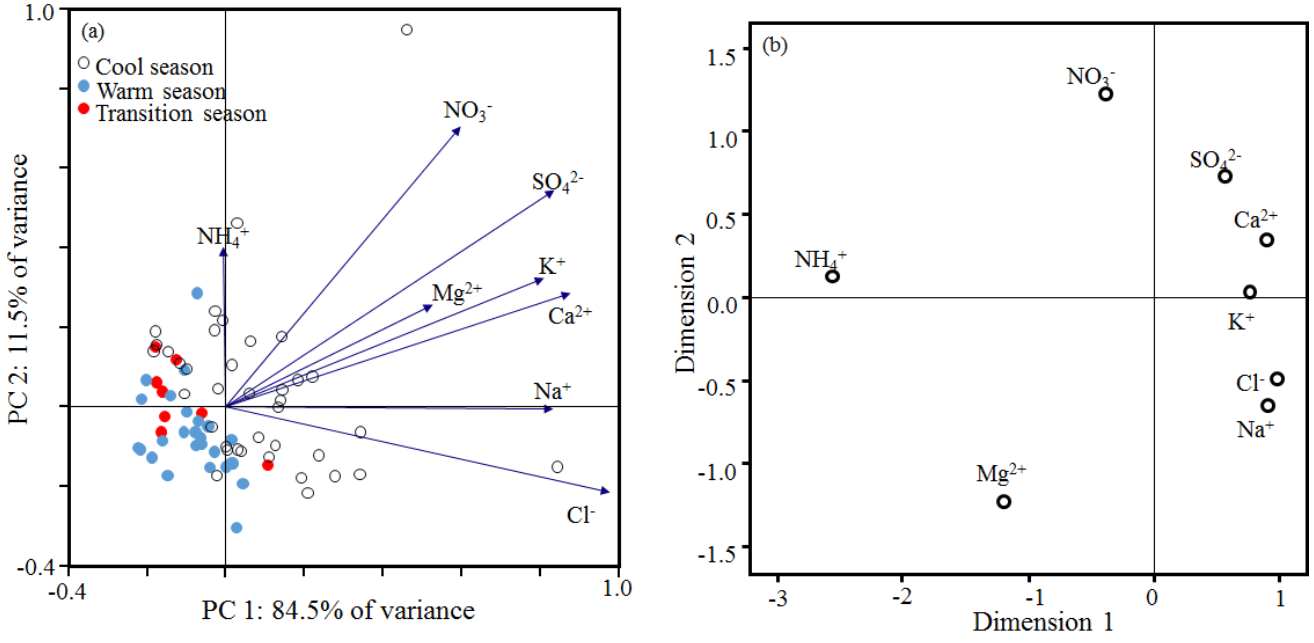

807

Atmos. Chem. Phys. Discuss., doi:10.5194/acp-2016-885, 2016
Manuscript under review for journal Atmos. Chem. Phys.
Published: 7 November 2016

Atmospheric Chemistry and Physics Discussions

808 **Figure 10** Ten-day back trajectories of warm (black, June through September 2014), cool (blue, March and April 2014 and October 2014 through February
809 2015) seasons, and transition season (red, May 2014) at Yongxing Island. Additionally, CWT (concentration weighted trajectory) plots for daily weighted-
810 average concentrations of TSP, Ca^{2+}, Mg^{2+}, K^{+}, SO_4^{2-}, NO_3^{-} and NH_4^{+} at Yongxing Island.

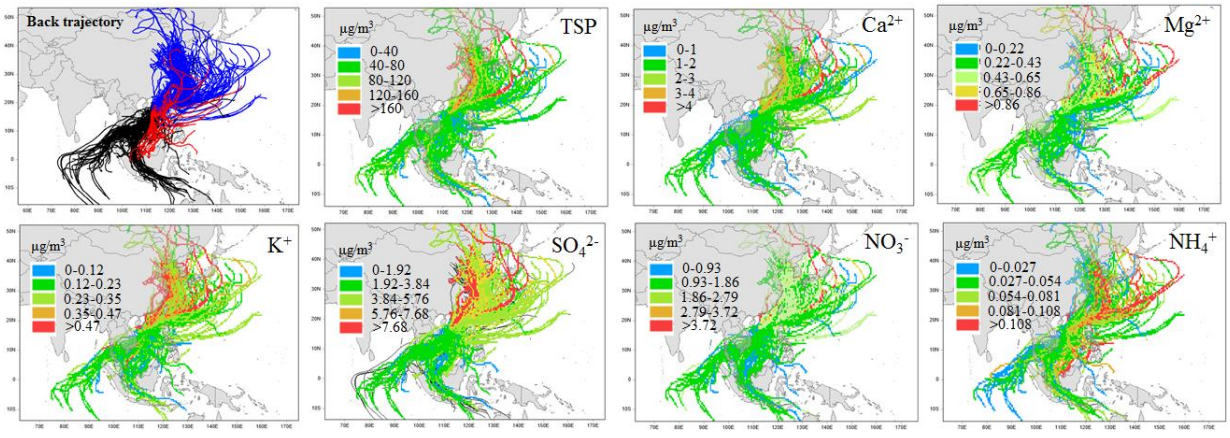

811